Published online 22 December 2011 *Nucleic Acids Research, 2012, Vol. 40, No. 8* ***3329–3347***
doi:10.1093/nar/gkr1232

Gli2 and MEF2C activate each other's expression and function synergistically during cardiomyogenesis *in vitro*

Anastassia Voronova, Ashraf Al Madhoun, Anna Fischer, Michael Shelton, Christina Karamboulas and Ilona Sylvia Skerjanc*

Department of Biochemistry, Microbiology and Immunology, Faculty of Medicine, University of Ottawa, Ottawa, Canada

Received July 25, 2011; Revised November 7, 2011; Accepted November 24, 2011

ABSTRACT

The transcription factors Gli2 (glioma-associated factor 2), which is a transactivator of Sonic Hedgehog (Shh) signalling, and myocyte enhancer factor 2C (MEF2C) play important roles in the development of embryonic heart muscle and enhance cardiomyogenesis in stem cells. Although the physiological importance of Shh signalling and MEF2 factors in heart development is well known, the mechanistic understanding of their roles is unclear. Here, we demonstrate that Gli2 and MEF2C activated each other's expression while enhancing cardiomyogenesis in differentiating P19 EC cells. Furthermore, dominant-negative mutant proteins of either Gli2 or MEF2C repressed each other's expression, while impairing cardiomyogenesis in P19 EC cells. In addition, chromatin immunoprecipitation (ChIP) revealed association of Gli2 to the *Mef2c* gene, and of MEF2C to the *Gli2* gene in differentiating P19 cells. Finally, co-immunoprecipitation studies showed that Gli2 and MEF2C proteins formed a complex, capable of synergizing on cardiomyogenesis-related promoters containing both Gli- and MEF2-binding elements. We propose a model whereby Gli2 and MEF2C bind each other's regulatory elements, activate each other's expression and form a protein complex that synergistically activates transcription, enhancing cardiac muscle development. This model links Shh signalling to MEF2C function during cardiomyogenesis and offers mechanistic insight into their *in vivo* functions.

INTRODUCTION

The mammalian heart is the first organ to develop and is essential for life. Perturbations in cardiogenesis can lead to congenital heart disease, the most prevalent birth defect worldwide. Heart development *in vivo* starts with the formation of the cardiac crescent, where the first heart field progenitor cells fuse to form the linear heart tube and give rise to the left ventricle. Second heart field progenitor cells then migrate to form pharyngeal and splanchnic mesoderm, which will form the right ventricle and the outflow tract (1,2). In order to properly define and maintain the cardiac identity, Sonic Hedgehog (Shh) signalling pathway members and myocyte enhancer factor 2 (MEF2) proteins are required as shown by various animal models [(3–10) and reviewed in ref. (1,2)].

In mammals, the Shh signal is transmitted into the cell by the patched1/smoothened (Ptch1/Smo) regulatory complex and is mediated by transcription factors glioma-associated factor (Gli) 1, 2, 3 [reviewed in refs (11,12)], which bind the TGGGTGGTC DNA consensus sequence (13). Gli1 acts as a transcriptional activator, but is dependent on Gli2- and/or Gli3-mediated transcription. Gli2 is a primary mediator of Shh signalling and functions mainly as a transcriptional activator. Gli3 is a transcriptional repressor (11). Using genetic inducible fate mapping, members of the Shh signalling pathway were shown to be expressed in murine myocardial progenitor cells starting from embryonic day (E) 7.0–8.0 (3). The expression of Gli1 in some atrial and ventricular myocytes was confirmed in another study when tamoxifen was administered to the $R26R^{Gli1\text{-}CreERT2}$ embryos at E6.5 (10). Thus, embryonic cardiomyocytes and/or cardiac progenitors were exposed to Shh signalling during development.

*To whom correspondence should be addressed. Tel: +1 613 562 5800 (Ext. 8669); Fax: +1 613 562 5452; Email: iskerjan@uottawa.ca

The Shh pathway participates in the establishment of a proper number of cardiac progenitor cells during early vertebrate heart development in zebrafish (3). Inhibition of the Shh signalling resulted in an early defect in myocardial progenitor specification leading to reduction of both ventricular and atrial cardiomyocytes (3). Additionally, activation of Shh signalling resulted in an increase of cardiomyocytes (3). The importance of the Shh signalling pathway in mammalian heart development was demonstrated by total and tissue-specific knockout studies. $Smo^{-/-}$ mice showed delayed formation of heart tube with delayed Nkx2-5 expression (4), whereas $Ptch1^{-/-}$ mice, where the negative regulation of Shh signalling was removed, demonstrated upregulated Nkx2-5 expression during heart development (4). Moreover, in $Shh^{-/-}$ mice there were atrial septal defects and aberrant development of the outflow tract (5). Additionally, $Gli2^{-/-}Gli3^{+/-}$ mice showed cardiac outflow tract anomalies (6,14). Tissue-specific removal of the Shh signalling pathway members in murine second heart field demonstrated their role in atrioventricular septation and the development of the outflow tract (8–10). In addition, Shh signalling was found to be important in proliferation of second heart field progenitors in chicken embryos (7). Therefore, Shh signalling via Gli2 is important for embryonic heart development.

In addition to Gli transcription factors, cardiomyogenesis is also regulated by MEF2 family members. The four vertebrate MEF2 proteins, MEF2A, MEF2B, MEF2C and MEF2D belong to the MADS box family (MCM1, Agamous, Deficiens, SRF) of transcription factors and bind A/T rich DNA sequence $(T/C)TA(A/T)_4TA(G/A)$ (15). MEF2C is the first MEF2 family factor to be expressed in heart myocardium progenitors starting from E7.5 (16,17).

Loss-of-function mutations in the single *Mef2* gene in *Drosophila* lead to a block of the development of all muscle cell types during embryogenesis (18). In mammalian embryogenesis, however, the four MEF2 family members play redundant roles and can rescue the phenotype resulting from a specific *Mef2* gene knockout [reviewed in ref. (15)]. For example, *Mef2c*-null mice undergo cardiomyogenesis but die from a failure to undergo heart looping morphogenesis and proper development of the right ventricle, as well as the outflow tract (19,20). Cardiomyogenesis might be occurring due to a 7-fold increase in MEF2B protein observed in *Mef2c*-null mice, which can partially compensate for the phenotype. Overlapping functions of MEF2C and MEF2B are also supported by the evidence of normal development of *Mef2b*-null mice (19). The possibility of the phenotype rescue by other MEF2 family members was eliminated by expression of a dominant-negative fusion protein, of MEF2C with the engrailed repression (EnR) domain (MEF2C/EnR) under the control of the Nkx2-5 enhancer that resulted in a severe disruption of cardiomyogenesis in mice (21). Thus, both Shh signalling and MEF2 family proteins play an important role in cardiomyogenesis *in vivo*.

The results from *in vivo* experiments have largely been reproduced *in vitro*. First, members of the Hedgehog signalling pathway and MEF2 transcription factors are expressed during cardiomyogenesis in embryonic stem (ES) cells (22–25). During cardiomyogenesis in mouse ES (mES) cells, committed cardiac progenitor cells express MEF2C and GATA-4 transcription factors after the formation of the mesodermal cells as characterized by the expression of Brachyury T (BraT) and Oct-4. Cardiac progenitor cells terminally differentiate into cardiomyocytes and express contractile proteins such as myosin heavy chain (MHC) and cardiac Troponin T (22).

A similar pattern of gene expression to ES cells can be seen in studies using pluripotent P19 embryonal carcinoma (EC) cells (26–28). The P19 EC cells were originally isolated from an induced teratocarcinoma of male mouse testes by injection of isolated mES cells (26). These cells can contribute to tissues in live-born chimeric mice (29) and can undergo controlled differentiation into cardiac and skeletal muscle cells (up to 15%) *in vitro* when treated with dimethylsulphoxide (DMSO) (27,28,30–34). We have previously shown that retinoic acid regulates skeletal myogenesis in P19 EC, mouse and human ES cells through upregulation of Pax3/7-positive progenitor cells (35,36), similar to a role for retinoic acid and Pax3/7 progenitors during embryogenesis (37,38). Moreover, Nkx-MEF2C/EnR was found to abrogate cardiac myogenesis both during murine embryogenesis and in P19 EC cells (21). Similarly, Nkx/EnR impaired cardiac muscle formation *in vivo* (39) and in P19 EC cells (40). More recently, we found that skeletal myosin light chain kinase (MLCK) is important for skeletal myogenesis in mES and P19 EC cells, as well as in the activation of satellite cells via interaction and subsequent phosphorylation of the MEF2C protein (25). For Gli2 and MEF2C expression, previous publications demonstrate that the members of the Shh signalling pathway and MEF2 family members are expressed during cardiomyogenesis in P19 EC cells (41,42) and P19CL6 cells (43,44), as well as in cardiomyocytes derived from mES cells stably expressing the neomycin-resistance gene under the regulation of the cardiac α-MHC promoter (23). Therefore, P19 EC cells use similar pathways as those identified in the embryo, mouse and human ES cells and are a suitable model to study cardiac and skeletal myogenesis *in vitro*.

Gain-of-function experiments in P19 EC cells revealed that both Gli2 and MEF2C are able to induce cardiomyogenesis through the upregulation of Nkx2-5, GATA-4 and BMP-4 factors (41,45). Inhibition of Shh signalling *in vitro* resulted in aberrant cardiomyogenesis in P19 and P19CL6 cells (42,43). Surprisingly, the ubiquitous expression of MEF2C/EnR, driven by the *pgk* promoter, enhanced cardiomyogenesis in P19 cells, likely by binding and inhibiting Class II histone deacetylases (HDACs), resulting in the recruitment of non-cardiac muscle cells into the lineage (46). However, consistent with the gain-of-function experiments, the cardiac-restricted expression of MEF2C/EnR, driven by an *Nkx2-5* enhancer, ablated cardiomyogenesis in P19 EC cells (21), demonstrating that MEF2 factors, or genes regulated by MEF2, are essential for cardiomyogenesis. Therefore, Shh signalling members and MEF2 proteins are important for cardiomyogenesis in stem cells.

Although Gli2 and MEF2C activate myogenic differentiation programs in a similar fashion (41,45,47,48), and their physiological role in heart development is known [(3–6,18,21) and reviewed in ref. (15)], their detailed function and the mechanism of their regulation is unclear. In this article, we examined the relationship between Gli2 and MEF2C during mES and P19 EC cellular cardiomyogenesis. We have found that Gli2 and MEF2C regulate each other's expression and associate with their respective gene elements, as well as form a protein complex capable of synergizing on gene promoters. We therefore link, for the first time, the Sonic Hedgehog signalling pathway to the function of MEF2C protein during cardiomyogenesis *in vitro*.

METHODS

Transgenic mice

$Gli2^{+/-}$ heterozygous mice [obtained from Dr A. Joyner, Sloan-Kettering Institute, New York, NY, USA; (49)] were maintained on CD1 background. $Gli2^{-/-}$ homozygous mice were generated by crossing two $Gli2^{+/-}$ heterozygous mice.

mES cell culture

D3 mES cells (ATCC, # CRL-1934) were maintained as described in ref. (25,35). For differentiation, cells were aggregated in hanging drops containing 800 cells each for the first 2 days. After culturing aggregates in suspension for an additional 5 days, they were plated on tissue-culture grade adherent plates or 0.1%-gelatin covered coverslips for the remaining 2 days of the 9-day differentiation protocol.

P19 EC cell culture

P19 EC cells (ATCC, #CRL-1825) were cultured and differentiated in the presence of 1% DMSO as previously described (50). Briefly, cells were aggregated in the presence of DMSO for 4 days and formed aggregates were plated onto 0.1%-gelatin covered coverslips or adherent tissue-culture grade dishes. P19 EC cells overexpressing various factors including P19[Gli2], P19[MEF2C], P19[Control], P19[Gli/EnR], P19[MEF2C-TAP] and P19[TAP] cells were described elsewhere (25,47). P19[Nkx-MEF2C/EnR] cells stably overexpressing MEF2C/EnR under the regulation of the Nkx2-5 enhancer (within the region from −9435 to −7353 nt relative to Nkx2-5 transcriptional start site) were described in ref. (21).

Immunofluorescence

On Day 6 of P19 EC and Day 9 of mES cell differentiation, cultures were fixed and incubated with MF20 monoclonal antibody supernatant to detect expression of MHC as previously described (50). Cy3-conjugated secondary antibodies (Jackson Immuno Research Laboratories, USA) were used to detect immunofluorescence (IF) as described in ref. (51). Hoechst dye was used as a nuclear marker. Indirect IF was captured using a Leica DMI6000B microscope (Leica Microsystems GmbH, Germany) or a Zeiss Axioscope microscope (Carl Zeiss MicroImaging GmbH, Germany). Images were collected at ×200 or ×400 magnification using Hamamatsu Orca AG camera (Hamamatsu Photonics, Germany) or Sony 3CCD camera (Sony Corporation, Japan) and processed using Velocity 4.3.2 (Perkin Elmer, Canada) or Axiovision (Carl Zeiss MicroImaging GmbH, Germany) software.

Quantitative PCR analysis

Total RNA from differentiating mES and P19 EC cells was harvested using RNeasy Mini Kit (Qiagen, Canada) and analysed using real-time quantitative PCR (QPCR) as described in refs (35,52). Briefly, 1 μg of RNA was reverse-transcribed (RT) to synthesize cDNA using Quantitect Reverse Transcription Kit (Qiagen, Canada). To ensure successful removal of genomic DNA, no-RT reaction was included. One-twentieth of RT reaction was used as a template for QPCR amplification using specific primers listed in Table 1 and the FastStart SYBR Green kit (Roche Applied Sciences, Canada) or Promega GoTaq QPCR Master Mix (Promega, WI, USA). Data were acquired using ABI7300 and ABI7500 QPCR (Applied Biosystems, CA, USA) or Eppendorf Realplex2 (Eppendorf, Canada) instruments. Data were normalized to β-actin, analysed as described in ref. (53), using P19 or P19 control cell line Day 0 (monolayer cultures) as a calibrator, and expressed as percent maximum. Data

Table 1. Oligonucleotide sequences of primers utilized for real-time QPCR

Target	Forward primer	Reverse primer
β-actin	AAATCGTGCGTGACATCAAA	AAGGAAGGCTGGAAAAGAGC
BraT	CTGGACTTCGTGACGGCTG	TGACTTTGCTGAAAGACACAGC
GATA-4	AAAACGGAAGCCCAAGAACCT	TGCTAGTGGCATTGCTGGAGT
Gli1	CCAAGCCAACTTTATGTCAGGG	TCCTAAAGAAGGGCTCATGGTA
Gli/EnR	GGAGAGTGTGGAGGCCAGTA	CTGGGTTCCGGCTGTCTCT
Gli2	CAACGCCTACTCTCCCAGAC	GAGCCTTGATGTACTGTACCAC
MEF2C	TCTGTCTGGCTTCAACACTG	TGGTGGTACGGTCTCTAGGA
MHC6	CAACAACCCATACGACTACGC	ACATCAAAGGGCCACTATCAGTG
Nkx2-5	AAGGAACAGCGGTACCTGTC	GCTGTCGCTTGCACTTGTAG
Oct-4	CAGCCAGACCACCATCTGTC	GTCTCCGATTTGCATATCTCCTG
Ptch1	AAAGAACTGCGGCAAGTTTTTG	CTTCTCCTATCTTCTGACGGGT
Tbx5	CTTTCGGGGCAGTGATGAC	TTGGATGAGGTGGAGAGAGC

represent mean ± standard error of mean (SEM) from at least two independent biological experiments and using two clonal populations per cell line.

Northern blot analysis

RNA from differentiating P19 and P19[Nkx-MEF2C/EnR] cells was harvested using the LiCl/Urea method and analysed using northern blot procedure as described previously (50). Briefly, a total of 12 µg of RNA for each sample was separated by denaturing gel electrophoresis and transferred to Hybond-N nylon membranes (GE Life Sciences, Canada). The membranes were hybridized with α-^{32}P deoxycytidine 5′-triphosphate labelled MEF2C/EnR and 18 S cDNA fragments described previously (21). Results shown are representative of three separate clones for each cell line.

Immunoblot analysis

Total protein extracts from differentiating mES and P19 EC cells and whole eyes of E16 Gli2$^{+/-}$ heterozygous and Gli2$^{-/-}$ homozygous mice were harvested using radioimmunoprecipitation assay buffer. In total, 10–20 µg of protein was resolved using 4–12% gradient NUPAGE gels (Invitrogen, Canada) according to manufacturer's protocol using 3-(N-morpholino)propanesulfonic acid/sodium dodecyl sulfate running buffer. Resolved proteins were transferred to polyvinylidene fluoride or nitrocellulose membranes, blocked in 5% milk and reacted with Gli2 (54), calmodulin binding protein (CBP) (Millipore, MA, USA), MEF2C (Santa Cruz, sc-13266), α-tubulin (Sigma, DM1A) or β-actin specific (Sigma, AC-74) antibodies. Signal was detected using HRP-conjugated secondary anti-rabbit (Millipore, MA, USA), anti-mouse (Cell Signalling, MA, USA) or anti-goat (Santa Cruz, sc-2020) antibodies.

ChIP assays

A quantity of 50 µg of chromatin from Day 5 differentiating P19[MEF2C] cells and 150 µg of chromatin from Day 4 differentiating P19[Gli2] cells was immunoprecipitated using 2 µg of MEF2C specific (Santa Cruz, sc-13266), Gli2 specific (Santa Cruz, G-20) or goat IgG non-specific antibodies (Invitrogen, Canada) as described in ref. (51). Briefly, cells were cross-linked with 4% formaldehyde (Fisher Scientific, Canada) and chromatin was sheared as described in ref. (51). Sheared chromatin was incubated with Gli2, MEF2C or IgG antibodies and the immune complexes were captured using protein G sepharose beads as described previously (51). Gli2, MEF2C or IgG-bound chromatin was quantified as a percent chromatin input using QPCR analysis as described above. To be considered a true association, each ChIP sample was examined for the enrichment of a chromatin locus immunoprecipitated with a specific antibody and compared with the same chromatin locus immunoprecipitated with a non-specific IgG (ANOVA with $P < 0.05$), and compared with a negative control locus, such as the *Ascl1* (55) or *Hdac4* locus (ANOVA followed by post hoc Tukey honestly significant difference (HSD) test with $P < 0.05$). Data represent mean ± SEM from three independent biological experiments. Primers are listed in Table 2.

Co-immunoprecipitation assays

HEK-293 cells (ATCC, #CRL-1573) were seeded at 1 million cells per 100 mm tissue-culture grade dish and 24 h later co-transfected with a total amount of 3 µg of

Table 2. Oligonucleotide sequences of primers utilized for ChIP–QPCR experiments

Target gene	Position of BS in mm9 genome	Strand Orientation	Forward primer	Reverse primer
Mef2c A	Chr13: 83556197 - 83556209	+	TGAAAAAGGAAATATCCCACTTAGA	TTGCATGGGTTCACACCTAA
Mef2c B	Chr13: 83589537 - 83589549	+	AGTTGCCTGAGCCTGTTTTC	TTTTTCGGCAATGATTTTCC
Mef2c C	Chr13: 83657044 - 83657056	+	TCTCCAGTTCCTGGGAAGAA	CTTTCGGCTGGAGAGTCTTG
Mef2c D	Chr13: 83663947 - 83663935	+	ACACACGCACACTTCGTCTC	GACCCACACAGAACCTTCAAA
Mef2c E	Chr13: 83734849 - 83734861	+	TTCCCATTTGGACCATTACC	ACCCACGCACTGAGACTTTC
Mef2c F	Chr13: 83772819 - 83772831	+	AACCCCAATCTTCTGCCACT	AAGCTTTCGCTAGACGTGGA
Mef2c G	Chr13: 83800500 - 83800512	+	GAGCCCCCTCTCTAATGTCC	TGTGGGCAAGTGTCTTTCTG
Mef2c H	Chr13: 83803968 - 83803980	+	CGACCGACCTGCTTTACTTG	AAGTGACATTTGGGGGTCCT
Mef2c I	Chr13: 83879226 - 83879238	+	CCTCCCCTCTTGTCAAAGTGT	CCTAATTATTTCAGTTTGGGATGC
Ptch1 A	Chr13: 63667821 - 63667833	−	TATTGCATGCGAGAGGGTTG	GGAGGGCAGAAATTACTCAGC
Gli1 A	Chr10: 126778677 - 126778689	−	GCACCCCCTCTCTAGCTTCTATC	GGACCACCCGCGAGAAGCGCAAACT
Ascl1 A	Chr10: 86936603 - 86936615	−	CCTAAGATCAATGGGCCAAA	CCCACCCAACTGTCCTAGAG
Gli2 A	Chr1: 120906302 - 120906324	−	AACAGGGTCTCTTCACATAGCC	ATCTGCGGAGCACCTACTGT
Gli2 B	Chr1: 120887621 - 120887643	−	GCATTTCTAAAGCTTGGTGGA	CCGTGTTAAACATGACTAAAATGAT
Gli2 C	Chr1: 120827230 - 120827246	−	TGAGTTATTGTTGGCGACTTCA	AAACTGGTGTGCTGGCTAGG
Gli2 D	Chr1: 120812203 - 120812225	−	CCCATTAACCACTGCTTTGC	GCTATATTTTCCTATTCATGGCATAC
Gli2 E	Chr1: 120799022 - 120799034	−	CTTCCCTGGGCCATTAAAGT	TGCTAATACTCCCAGGCACA
Gli2 F	Chr1: 120796554 - 120796566	−	TGCCCTAATTACACAAACAGCA	CCTACTAATAACCTCCATGGATCA
Gata-4 A	Chr14: 63864687 - 63864697	+	AAGCGCTCTTTTCTCCTTCC	GTGAGGGCTACAGGGAGTGA
MyoG A	Chr1: 136186098 - 136186104	+	ATTTGCCCTTCTGGGTTTCT	GCTCAGCAGCACCTTAAACC
Hdac4 A	Chr1: 93901621 - 93901643	+	ATCTCCCACTGTTGGTCTGC	GGTTTTCACTTTGTGGATTTGG

Chr: chromosome; BS: binding site.

Gli2, MEF2C-Flag or Flag-vector (DYKDDDDK flag peptide) using Fugene (Roche, Canada). On completing 24 h post-transfection, cells were washed twice with ice-cold phosphate buffered saline and lysed with buffer containing 50 mM Tris–HCl, pH 7.4, 150 mM NaCl, 1 mM EDTA and 1% Triton X-100. Lysates were clarified by centrifugation for 15 min at 13 krpm. In total, 0.5 mg of protein was subjected to FLAG immunoprecipitation (IP) according to manufacturer's protocol (Sigma-Aldrich, MO, USA). Bound proteins were eluted by boiling the beads in 1 × SDS–PAGE loading buffer for 10 min at 95°C. Transfection efficiency was monitored by co-transfecting Green fluorescent protein (GFP) and analysing its autofluorescence. All protein extraction and incubation procedures were carried out at 4°C in the presence of 1× protease inhibitor cocktail (Roche, Canada) and 0.5 mM phenylmethanesulphonylfluoride (PMSF).

Eluted proteins from co-immunoprecipitation assays in HEK-293 cells were resolved using 4–12% gradient NUPAGE gels, transferred to polyvinylidene fluoride membranes and reacted with Gli2- or MEF2C-specific antibodies as described above. Gli2 purification efficiency was quantified by band densitometry analysis using ImageJ program (56).

Reporter assays

Gli2, MEF2C-Flag and GATA-4 expressing plasmids are described elsewhere (25,47,57). Gli-responsive promoter is described in ref. (58) and MEF2-responsive promoter is from Affymetrix, CA, USA. The Nkx2-5 promoter, comprising −3059 to +223 nt relative to the Nkx2-5 transcriptional start site, termed Nkx2-5-luc, is described in Ref. (59).

P19 EC cells were plated at a density of 150 000 cells/35 mm tissue-culture grade dish and transiently co-transfected, as described above, 24 h later with a total amount of 3 μg of DNA with or without Gli2, MEF2C-Flag and the Nkx2-5 promoter, Gli-responsive promoter or MEF2-responsive promoter driving luciferase gene in the ratio 2 : 1 relative to luciferase reporters. Transfection efficiency was monitored by transfecting *Renilla* as described previously (51). On completing 24 h after transfection, cells were washed twice with ice-cold phosphate buffered saline and lysed according to Dual Luciferase Kit protocol (Promega, WI, USA). Luciferase activity was assayed using 10–15 μl of lysate and LmaxII384 luminometer (Molecular Devices, USA). To remove the background, the normalized activity of the luciferase reporter plasmid alone was subtracted from its activity in the presence of Gli2 and/or MEF2C and GATA-4. The activity of the luciferase reporter in the presence of protein expression plasmids was normalized to the activity in the presence of Gli2 (arbitrarily set at 1). Synergy was calculated as described in ref. (60) according to the following formula:

$$\text{Synergy} = \frac{\text{RLUs(MEF2C+Gli2)}}{\text{RLUs(MEF2C)+RLUs(Gli2)}},$$

where relative luciferase units (RLUs) represent luciferase activity normalized to *Renilla* activity. P19 cells transfected with GATA-4 and Nkx2-5-luc in ratio 2:1 served as a positive control.

Bioinformatics analysis

Conserved Gli DNA binding sites and MEF2 DNA binding sites in the *Mef2c* and *Gli2* genes (± 100 kb) were identified using Mulan (Multiple Sequence Local Alignment and Visualization tool) as described previously (61). The primers for identified binding sites were designed using Primer 3 software (62) (for primer sequences, see Table 2).

Putative genomic targets for both Gli and MEF2 transcription factors were identified using SynoR (Genome miner for synonymous regulation) as described previously (63). The distance between neighbouring DNA binding sites was set to (i) 4–100 bp; (ii) 100–200 bp and (iii) 200–300 bp. The mouse genome (mm9) was used as a base and was compared with the human genome (hg18). Identified genes are listed in Supplementary Table S1. Functional annotation analysis of the identified potential targets was performed using DAVID (Database for Annotation, Visualization, and Integrated Discovery) software as described in Refs. (64,65). Selected gene ontology biological processes are listed in Table 3.

Statistical analysis

ANOVA followed by post hoc Tukey HSD test was performed using XLSTAT11 software (Addinsoft, NY, USA) to determine statistical significance between mean values of two groups ($^*P < 0.05$; $^{**}P < 0.01$).

RESULTS

Gli2 and MEF2C are expressed during cardiomyogenesis in mES and P19 EC cells

Differentiation of mES cells into cardiac muscle is schematically depicted in Figure 1A, using a 7-day aggregation protocol (25), where cardiac muscle forms as early as Days 8–9 (Figure 1A). Formation of cardiac muscle from mES cells was confirmed by indirect IF with an anti-MHC antibody, MF20 (Figure 1B).

Changes in gene expression during cardiomyogenesis in mES cells were examined for several markers (Figure 1C). Downregulation of Oct-4, a marker of pluripotency in ES cells (66), confirmed that mES cells differentiated efficiently (Figure 1C, panel Oct-4). Notably, a slight upregulation of Oct-4 was observed on Day 3, in agreement with a previously reported role for Oct-4 in cardiac mesoderm formation (67). The mesodermal marker BraT (68), was also upregulated on Day 3 of mES differentiation (Figure 1C, panel BraT). The highest expression of the cardiac muscle precursor transcription factors Tbx5, Nkx2-5 and GATA-4 (69–71) was detected during Days 6–9 of mES differentiation (Figure 1C, panels Tbx5, Nkx2-5 and GATA-4). Finally, the highest expression of the cardiac muscle marker MHC6 was detected on Day 9 of mES differentiation (Figure 1C, panel MHC6). During

Table 3. Selected gene ontology biological processes significantly enriched among genes containing Gli and MEF2 conserved DNA binding clusters in UTR, promoter, intron and coding sequence regions

Category	Targets	Fisher's exact *P*-value	Example genes
Cellular process	562	2.1E-17	E2F4, Glis1, CCNB2, Hdac9, RBBP4, TCF4
System development	189	6.1E-19	Tbx15, Fgf10, GSK3b, VEGFC, Sox6, Bmp1, Ar
Regulation of gene expression	172	6.4E-7	DNMT3A, POU4F2, Smarcc2, FOXA2, FOXD3, HOXD10, Lhx2, Pbrm1
Cell differentiation	143	4.5E-13	ANGPT1, Bmp7, Fgf1, PAX2, Ptch1, Hhip, Twist1
Nervous system development	99	3.3E-15	BDNF, NRXN1, FOXP2, Gfra1, HOXB3
Embryonic development	68	3.5E-8	Notch2, Pdgfra, Pcgf2, HOXD10, ITGA8, Nr4a3
Neurogenesis	60	8.5E-9	Ntng1, NAV1, Lhx8, APP, Ctnna2
Skeletal system development	31	9.1E-5	Bmp5, Sox5, HOXB8, Tapt1
Chromatin organization	31	5.2E-4	MYST4, Phf15, ASH1L, ING2, Rnf2
Heart development	27	4.9E-5	MEF2C, FOXP1, TTN, Hdac5, ALPK3
Muscle organ development	17	1.5E-2	Dmd, Utrn, Rora, CACNG2
Vascular smooth muscle contraction	16	5.1E-4	Cacna1C, Cacna1D, BRAF, Prkca

For complete list of genes, see Supplementary Data. Altogether, 957 potential target genes were analysed as described in 'Materials and Methods' section. The background set of genes used was the entire mouse genome.

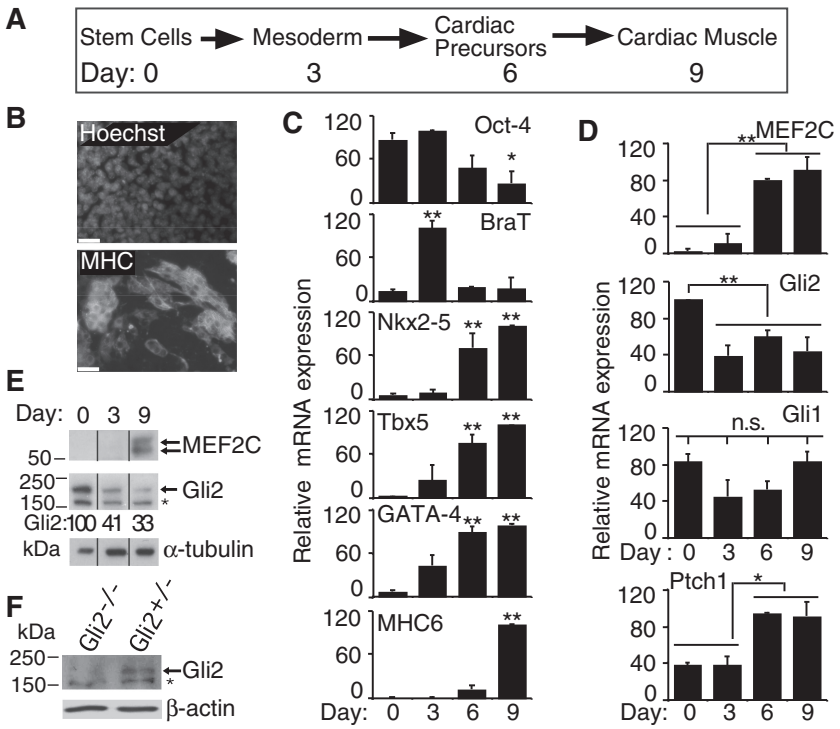

Figure 1. Gli2 and MEF2C are expressed during mES differentiation. (**A**) Schematic representation of cardiomyogenesis in D3 mES cells, as described in 'Materials and Methods' section. (**B–E**) mES cells were differentiated and examined (B) for MHC expression using MF20 antibodies on Day 9 of differentiation. Nuclei were stained with Hoechst, scale bar is 30 μM; (C and D) by QPCR analysis for the indicated genes on Days 0, 3, 6 and 9 of differentiation, $n = 3$. Error bars represent ± SEM. Primers are listed in Table 1. (C) Values were compared with Day 0 values and statistical significance was determined using ANOVA ($*P < 0.05$ and $**P < 0.01$). (D) To determine statistical significance between all days analysed, ANOVA followed by post hoc Tukey HSD analysis was performed, $*P < 0.05$ and $**P < 0.01$; n.s. = not significant.; (E) immunoblot analysis of total protein extracts using MEF2C- and Gli2-specific antibodies at the time shown. Arrows designate Gli2 or MEF2C protein band(s), and asterisk denotes non-specific binding of the Gli2 antibodies. α-Tubulin served as a loading control. Lanes were spliced out from the same autoradiogram as designated by vertical lines. Gli2 band densities were measured from one representative experiment using ImageJ program (56), normalized to α-tubulin and expressed as percent maximum; (**F**) immunoblot analysis of eye total protein extracts from E16 $Gli2^{+/-}$ and $Gli2^{-/-}$ mice using Gli2-specific antibodies. Asterisk denotes non-specific binding of the antibodies. β-Actin served as a loading control.

mES differentiation, MEF2C mRNA levels became highly upregulated starting from Day 6 (Figure 1D, MEF2C panel), whereas Gli2 mRNA levels were downregulated starting from Day 3 (Figure 1D, Gli2 panel). There was a trend in Gli1 mRNA downregulation on Days 3–6 of differentiation (Figure 1D, panel Gli1). In contrast, Ptch1

mRNA was upregulated on Days 6–9 of mES differentiation (Figure 1D, panel Ptch1). MEF2C and Gli2 protein expression levels correlated with their mRNA expression levels (Figure 1E). MEF2C protein expression was induced after Day 3 of differentiation and Gli2 protein expression was downregulated after Day 3, although its expression persisted until Day 9 (Figure 1E).

To confirm that the upper band on the Gli2 immunoblot did indeed correspond to Gli2 protein, we analysed whole eye total protein extracts from $Gli2^{+/-}$ heterozygous and $Gli2^{-/-}$ homozygous mice. The only band absent in the $Gli2^{-/-}$ protein sample was the upper band corresponding to ~180 kDa (Figure 1F). Thus, the upper band represents Gli2 that correlates well with previously published data (54,55) and with the theoretical molecular weight of 165 kDa for full-length mouse Gli2 protein (database accession number Q0VGV1). Therefore, both Gli2 and MEF2C proteins were expressed during mES cell cardiomyogenesis (summarized in Table 4).

Since mES cells spontaneously differentiate into cell types of all three germ layers upon removal of leukemia inhibitory factor (77) and only a small proportion of cells differentiate into cardiac muscle using a standard embryoid body differentiation protocol, it is difficult to specifically correlate the expression profile of MEF2C and Gli2 with cardiac myogenic differentiation in a heterogeneous population of mES cells. P19 EC cells, in contrast, mainly differentiate into mesoderm and endothelial lineages upon addition of DMSO (27,30–34). Moreover, P19 EC myogenic differentiation is very similar to mES myogenic differentiation (25,35). For these reasons, we compared the expression pattern of Gli2 and MEF2C during mES differentiation with DMSO-induced differentiation of P19 EC cells.

Cardiomyogenic differentiation of P19 EC cells is schematically presented in Figure 2A. P19 EC cells treated with DMSO successfully differentiated into cardiac muscle on Day 6 as observed by indirect IF using MHC-specific antibodies (Figure 2B). Gene expression changes during cardiomyogenesis in P19 EC cells were followed by QPCR analysis of myogenic markers (Figure 2C). Downregulation of Oct-4 starting from Day 2 indicated the loss of pluripotency in EC cells (Figure 2C, panel Oct-4). Induction of mesoderm is indicated by the robust upregulation of BraT expression on Day 2 of differentiation (Figure 2C, panel BraT). Induction of cardiomyogenesis was confirmed by elevated expression of Nkx2-5, Tbx5 and GATA-4 during Days 5–6 of P19 EC differentiation (Figure 2C, panels Nkx2-5, Tbx5 and GATA4). The robust expression of MHC6 on Day 6 of differentiation confirmed the formation of cardiac muscle in EC cells (Figure 2C, panel MHC6). The expression of MEF2C mRNA was significantly elevated ($P < 0.01$) during Days 5–6 of DMSO-induced differentiation of P19 EC cells (Figure 2D, panel MEF2C), and resembled the temporal pattern observed in mES cells (Figure 1D, panel MEF2C). There was a significant increase ($P < 0.05$) in Gli2 mRNA expression during Days 5–6 of P19 EC cardiomyogenesis (Figure 2D, panel Gli2). Gli1 mRNA was upregulated on Day 4 of differentiation (Figure 2D, panel Gli1). This data correlates with previous reports showing upregulation of MEF2C and Gli2 mRNA expression during P19 EC DMSO-induced myogenesis using northern blot analysis (35,41,42,47,51,78). Therefore, MEF2C and Gli2 transcription factors are expressed during mES and P19 EC cell cardiomyogenesis (summarized in Table 4).

Gli2 regulates expression of MEF2C during cardiomyogenesis in P19 EC cells

To study the ability of Gli2 to regulate the expression of MEF2C during cardiomyogenesis in stem cells, we examined P19 cells that stably overexpressed Gli2 (Figure 3). Stable overexpression of Gli2 was confirmed

Table 4. Summary of gene expression changes in cell lines treated with or without DMSO

Cell line	Treatment	BraT	Nkx2-5	GATA-4	Tbx5	MHC6	Gli2	MEF2C	References
mES	–	+D3	+D6–9	+D6–9	+D6–9	+D9	+highest on D0	+D6–9	Figure 1 (72,73)
P19	DMSO	+D1–3	+D4–6	+D3–6	+D4–6	+D5–6	+D4–6	+D4–6	Figure 2 (27)
P19[Gli2]	DMSO	±D2	++D6	++D6	++D6	++D6	+++D0–6	++D4–9	Figure 3
P19[MEF2C-TAP]	DMSO	+D2	++D6	++D6	+D6	+D6	++D4–5	+++D0–6	Figure 3
P19[Gli/EnR]	DMSO	+D0–9	±D4–6	±D4–6	±D4–6	±D4–6	+D0–9	±D4–6	Figure 4 (47,51)
P19[Nkx-MEF2C/EnR]	DMSO	+D2–6	±[a]D0–6	−D0–6	−D6	−D6	±D6	±[a]D0–6	Figure 5 (21)
P19[Nkx/EnR]	DMSO	++D2–4	N.D.	−D0–4, D6	N.D.	N.D.	N.D.	−D6	(40)
P19[β-cat/EnR]	DMSO	±D0-9	N.D.	N.D.	N.D.	N.D.	−D0-9	N.D.	(74)
P19[Pax/EnR]	DMSO	++D0–9	N.D.	+D9	N.D.	N.D.	+D0–9	N.D.	(75)
P19[Meox/EnR]	DMSO	+D0–9	+D6	+D6	N.D.	N.D.	±D0–9	N.D.	(47; Petropoulos and Skerjanc, unpublished data)
P19[MyoD/EnR]	DMSO	N.D.	N.D.	−D9	N.D.	N.D.	±D9	−D9	(76)
P19[EnR]	DMSO	+D0–6	+D0–6	+D0–6	N.D.	N.D.	+D0–6	+D0–6	(40)

[a]The expression of Nkx2-5 and MEF2C was elevated during Days 0–3, whereas it was downregulated during Days 4–6 of P19[Nkx-MEF2C/EnR] differentiation as compared with P19 control cells [ref. (21) and Figure 7C].

Cell lines indicated on the right were aggregated under the conditions described in 'Materials and Methods' section and the induction of muscle marker gene expression was monitored. (+++: high expression; ++: elevated expression; +: normal expression; ±: downregulated expression, −: not expressed or basal level of expression; N.D.: not determined). The timing of temporal gene expression in parental mES and P19 EC cells is shown. For stable cell lines, the change in expression relative to the respective control cell lines and the day examined, were indicated (D = day).

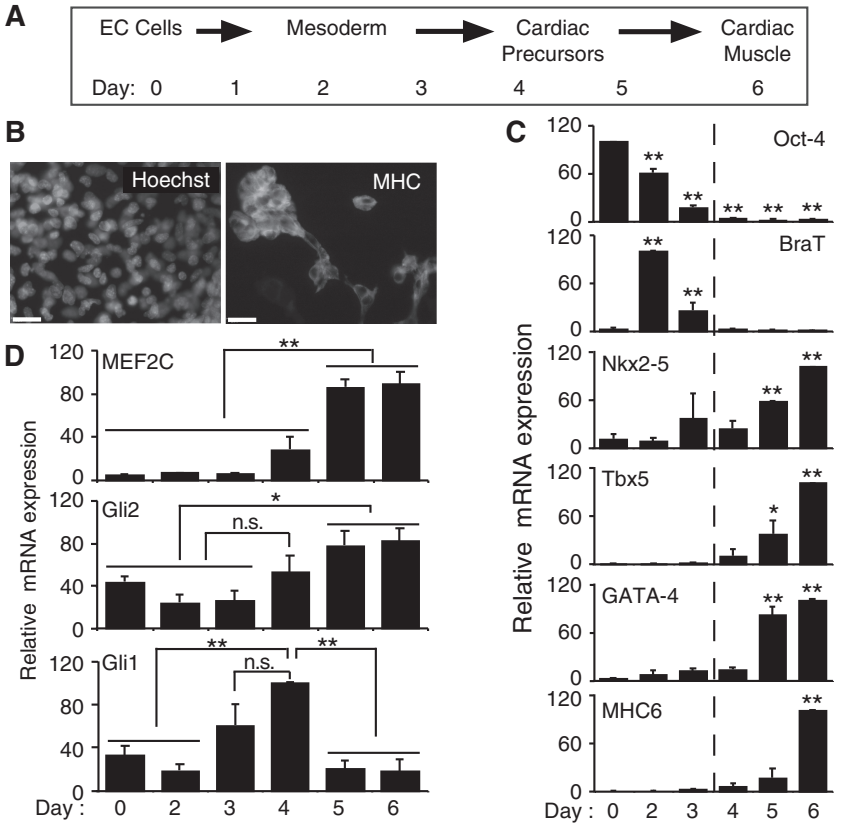

Figure 2. Gli2 and MEF2C are expressed during P19 EC DMSO-induced myogenesis. P19 EC cells were differentiated in the presence of 1% DMSO as described in 'Materials and Methods' section. (**A**) Schematic representation of cardiomyogenesis in P19 EC cells. (**B**) P19 cells were examined for MHC expression on Day 6 of differentiation using MHC-specific antibodies. Nuclei were stained with Hoechst dye. Scale bar is 30 μM; (**C** and **D**) QPCR analysis of the expression of the indicated genes at the times shown, $n = 3$. Error bars represent ± SEM. Primers are listed in Table 1; (C) Day 2–6 values were compared with Day 0 values and statistical significance was determined using ANOVA ($*P < 0.05$ and $**P < 0.01$); (D) to determine statistical significance between all days, ANOVA followed by post hoc Tukey HSD analysis was performed, $*P < 0.05$ and $**P < 0.01$; n.s. = not significant.

by immunoblot analysis using Gli2-specific antibodies (Figure 3A). Antigenic analysis using MHC-specific antibodies revealed an enhancement in the formation of cardiomyocytes in Day 6 differentiated P19[Gli2] cultures (Figure 3B and C). This was confirmed by QPCR analysis, which showed increased levels of Nkx2-5, Tbx5, GATA-4 and MHC6 mRNA in P19[Gli2] cells as compared with P19[Control] cells (Figure 3D, panels Nkx2-5, Tbx5, GATA-4 and MHC6) (summarized in Table 4). Enhancement of cardiomyogenesis by Gli2 is consistent with previous findings (3,41). Notably, overexpression of Gli2 resulted in a slight downregulation (15 ± 4%) of BraT expression on Day 2 of differentiation (Figure 3D, panel BraT). Furthermore, P19[Gli2] cells overexpressing Gli2 protein showed a statistically significant ($P < 0.05$) upregulation of MEF2C mRNA levels on Day 4 of DMSO-induced differentiation (Figure 3D, panel MEF2C), similar to results shown in the absence of DMSO (41). There was also an 11- to 20-fold upregulation of MEF2C protein levels in P19[Gli2] cells on Days 6–9 of DMSO-induced differentiation as compared to P19[Control] Day 4 (Figure 3A). The increases in MEF2C protein expression on Days 6–9 in P19 and P19[Gli2] cells (Figure 3A) correlate with the pattern of MEF2C mRNA expression in P19 cells (compare with Figure 2D), which peaks by Day 5. The increase in MEF2C mRNA on Day 4 in P19[Gli2] (Figure 3D) cells did not correlate with an obvious increase in MEF2C protein on that day (Figure 3A), possibly due to post-transcriptional regulation of the MEF2C protein [reviewed in ref. (15)]. Overall, overexpression of Gli2 upregulates MEF2C mRNA and protein expression while enhancing cardiomyogenesis (summarized in Table 4).

Since Gli transcription factors have overlapping functions both *in vivo* and *in vitro* (79–82), the use of a dominant negative fusion protein of Gli2 with the EnR domain (Gli/EnR) would result in repression of all Gli2-bound regulatory elements and the inability of Gli1 or Gli3 to rescue the phenotype. This approach has successfully been used previously both *in vitro* and *in vivo* (21,74,75,83,84). Furthermore, overexpression of Engrailed does not interfere with cardiomyogenesis in P19 EC cells (40). Stable overexpression of Gli/EnR (Figure 4C, panel Gli/EnR) resulted in the formation of fewer MHC-positive cardiomyocytes when compared with P19 control cells (Figure 4A and B). Downregulation of cardiac muscle cell differentiation was confirmed by lower

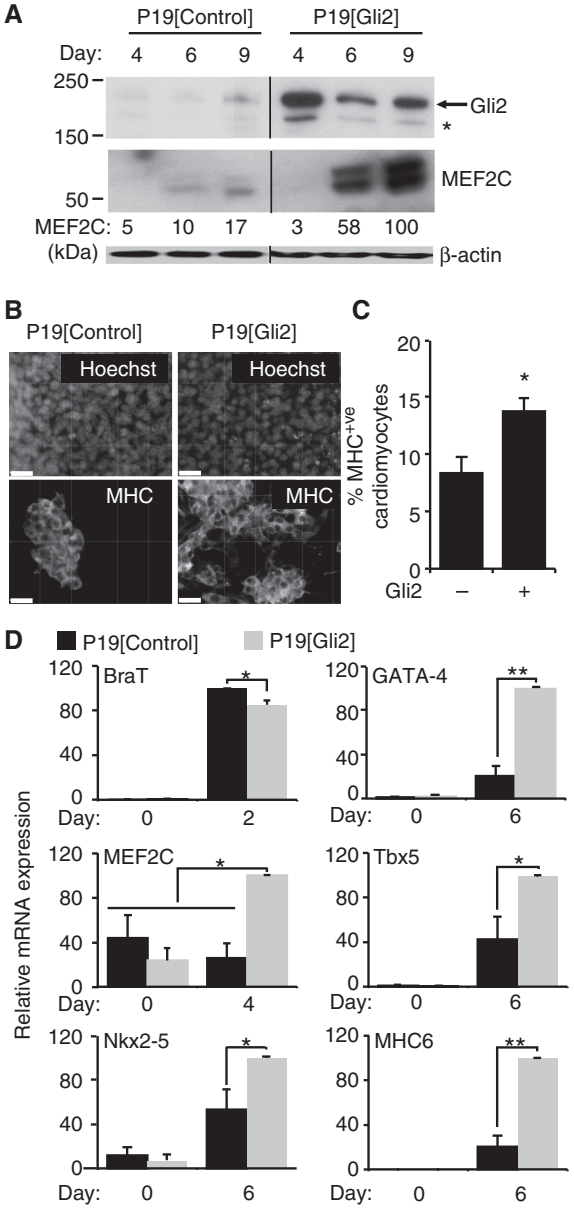

Figure 3. Gli2 upregulates MEF2C expression while enhancing cardiomyogenesis in P19 EC cells. P19[Gli2] and P19[Control] cell lines were differentiated in the presence of 1% DMSO. (**A**) Immunoblot analyses of Gli2 and MEF2C protein expression in differentiating P19[Control] and P19[Gli2] cells on Days 4, 6 and 9 using Gli2-specific or MEF2C-specific antibodies. Arrow designates Gli2 protein band and asterisk denotes non-specific binding of the Gli2 antibodies. β-Actin served as a loading control. Lanes were spliced out from the same autoradiogram as designated by vertical lines. MEF2C band densities from one representative experiment were measured using ImageJ program (56), normalized to β-actin and expressed as percent maximum; (**B**) Day 6 differentiated P19[Control] and P19[Gli2] cultures were reacted with MHC-specific antibodies. Nuclei were stained with Hoechst dye. Scale bar is 30 μM; (**C**) MHC-positive cardiomyocytes from (B) were counted in 10 random fields and expressed as percent of the total number of nuclei, $n = 4$. In total, 13 000 cells were counted; (**D**) QPCR analysis of the expression of the genes indicated at the times shown in P19[Control] (black bars) and P19[Gli2] (grey bars) cultures. Error bars represent ± SEM from two biological replicas of two clonal populations ($n = 4$). Statistical significance using an ANOVA test was determined between groups of P19[Control] and P19[Gli2] samples analysed on the same day. For MEF2C expression, ANOVA followed by post hoc Tukey HSD test was performed to determine statistically significant difference between P19[Control] and P19[Gli2] samples on all days analysed, $*P < 0.05$ and $**P < 0.01$. Primers are listed in Table 1.

expression of MHC6 (Figure 4C, panel MHC6). The mRNA levels of Tbx5 and GATA-4 were downregulated since Day 4, whereas levels of Nkx2-5 were downregulated most significantly ($P < 0.05$) on Day 6 of P19[Gli/EnR] cellular differentiation (Figure 4C, panels Tbx5, Nkx2-5 and GATA-4). MEF2C mRNA was downregulated in P19[Gli/EnR] cells on Days 5 and 6 of differentiation (Figure 4C, panel MEF2C). The effect of MEF2C downregulation is not due to global gene repression by Gli/EnR fusion protein since Gli/EnR did not greatly affect expression of mesodermal markers such as BraT in DMSO-induced differentiation (47) (Table 4). P19[Gli/EnR] cells did not lose pluripotency or the ability to differentiate as they were shown to differentiate into glial and neuronal cells in the presence of retinoic acid (55). Therefore, Gli2, or genes bound by Gli2, is essential for maintaining normal expression of MEF2C during cardiomyogenesis in P19 EC cells (summarized in Table 4).

Gli2 associates with *Mef2c* gene elements during cardiomyogenesis in P19 EC cells

In order to determine if Gli2 binds *Mef2c* gene elements during cardiomyogenesis, we performed ChIP experiments. *In silico* analysis of the *Mef2c* gene (± 100 kb) revealed nine conserved theoretical Gli binding sites (GBS) (*Mef2c* A–I, Figure 5A and B, summarized in Table 2), suggesting that MEF2C could be a target of a Gli transcription factor. Since the highest expression of Gli2 protein and of MEF2C mRNA was detected on Day 4 of P19[Gli2] cellular differentiation (Figure 3A and D, respectively), we performed ChIP analysis of Day 4 differentiating P19[Gli2] EC cells. After ChIP with a Gli2 antibody, a statistically significant enrichment was observed of chromatin fragments, corresponding to *Mef2c* sites B–I (Figure 5C). *Mef2c* site A appeared not to be associated with Gli2 protein (Figure 5C), therefore showing specificity of the ChIP assay. The *Gli1* and *Ptch1* promoter regions were used as positive controls and *Ascl1* gene element was used as a negative control (Figure 5C) based on previous observations (55,85,86). From this result, we observe for the first time that Gli2 is associated with *Mef2c* gene elements during cardiomyogenesis in P19 EC cells.

MEF2C regulates expression of Gli2 during cardiomyogenesis in P19 EC cells

To study the ability of MEF2C to regulate the expression of Gli2 during cardiomyogenesis *in vitro*, we examined P19 cells that stably overexpressed MEF2C-TAP [tandem affinity purification tag (25)] (Figure 6). Stable overexpression of MEF2C-TAP was confirmed by immunoblot analysis using CBP-specific antibodies that recognized the TAP-tag of the MEF2C-TAP protein (Figure 6A). Antigenic analysis using MHC-specific antibodies revealed an enhancement in cardiac muscle formation in P19[MEF2C-TAP] cells when compared with their respective control cells (Figure 6B and C). This is in agreement with previous findings, where MEF2C was shown to induce cardiomyogenesis in the absence of DMSO (45). We also observed significantly ($P < 0.01$)

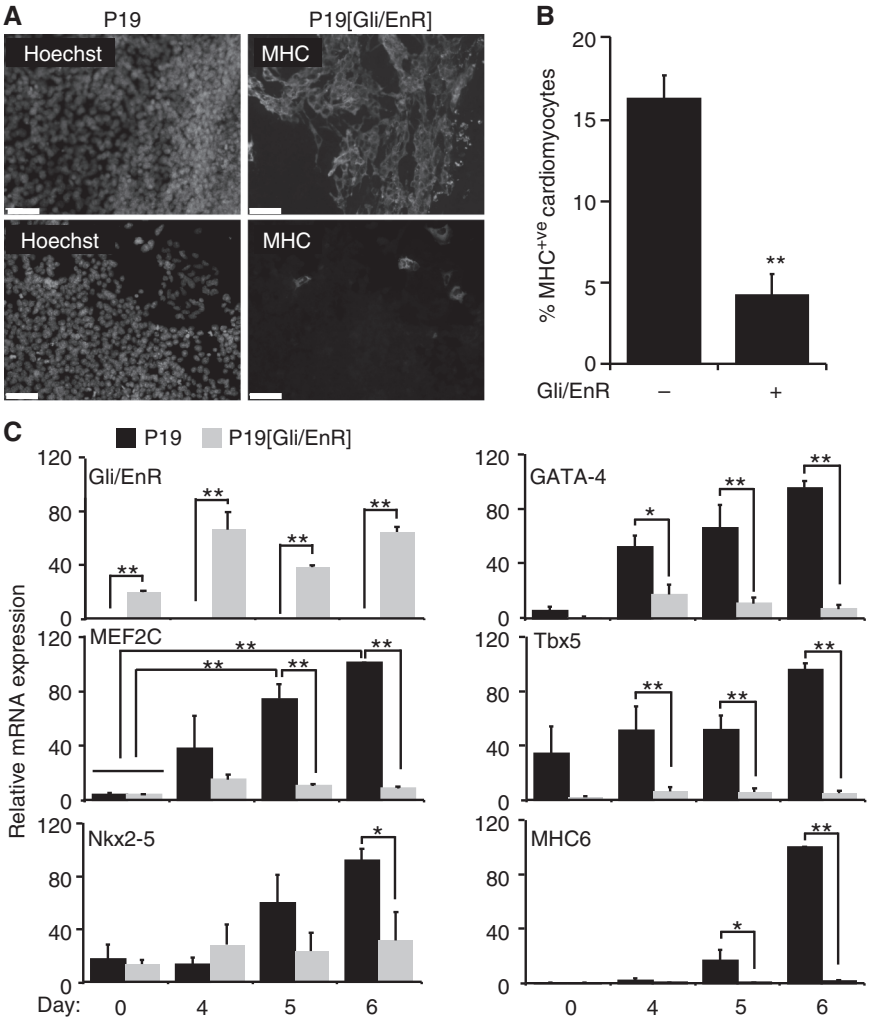

Figure 4. Expression of Gli/EnR downregulates MEF2C expression while downregulating cardiomyogenesis in P19 EC cells. P19 and P19[Gli/EnR] cell lines were differentiated in the presence of 1% DMSO. (**A**) Antigenic analysis of P19 and P19[Gli/EnR] using MHC-specific antibodies on Day 9 of differentiation. Nuclei were stained with Hoechst dye. Scale bar is 60 μM; (**B**) MHC-positive cardiomyocytes from (A) were counted in 10 random fields and expressed as percent of the total number of nuclei, $n = 4$. In total, 16 000 cells were counted; (**C**) QPCR analysis of the expression of the genes indicated on Days 0 and 4–6 in P19 (black bars) and P19[Gli/EnR] (grey bars) cultures. Error bars represent ± SEM from two biological replicas of two clonal populations ($n = 4$). Statistical significance using ANOVA test was determined between groups of P19 and P19[Gli/EnR] samples analysed on the same day. For MEF2C expression, ANOVA followed by post hoc Tukey HSD test was performed to determine statistically significant difference between P19 and P19[Gli/EnR] samples on all days analysed, $*P < 0.05$ and $**P < 0.01$. Primers are listed in Table 1.

increased levels of Nkx2-5 and GATA-4, as well as a trend of increased MHC6 transcripts in Day 6 differentiated P19[MEF2C-TAP] cultures as compared with their control cell line (Figure 6D, panels Nkx2-5, GATA-4 and MHC6). Notably, Tbx5 mRNA was not affected by the expression of MEF2C-TAP (Figure 6D, panel Tbx5). Also, expression of MEF2C-TAP did not affect BraT transcript levels, suggesting that MEF2C-TAP affects cardiomyogenesis after mesoderm induction (Figure 6D, panel BraT). Furthermore, overexpression of MEF2C-TAP resulted in the elevation of Gli2 mRNA expression on Day 4 of P19 EC differentiation (Figure 3D, panel Gli2). We also observed an increase in Gli2 protein levels up to 2.4-fold on Days 5 and 6 of P19[MEF2C-TAP] differentiation as compared with Day 5 of differentiation in P19[TAP] cells (Figure 6A). Therefore, MEF2C upregulates Gli2 expression while enhancing cardiomyogenesis in P19 EC cells (summarized in Table 4).

To test if the expression of Gli2 can be regulated by a dominant-negative MEF2C, we examined P19 EC cells expressing MEF2C/EnR under the regulation of the *Nkx2-5* enhancer (Figure 7A). As reported previously (21), P19[Nkx-MEF2C/EnR] cells failed to undergo cardiomyogenesis as evidenced by the absence of MHC-positive cardiac muscle cells (Figure 7B) and a severe downregulation of Nkx2-5, Tbx5, GATA-4 and MHC6 mRNA (Figure 7C, panels Nkx2-5, GATA-4, Tbx5 and MHC6). The phenotype of P19[Nkx-MEF2C/EnR] cells is in accordance with previous reports showing complete absence of cardiomyogenesis *in vivo* or in P19 EC cells (21). Expression of Nkx-MEF2C/EnR affected cardiomyogenesis only, as differentiating P19[Nkx-MEF2C/EnR] cells showed normal upregulation of

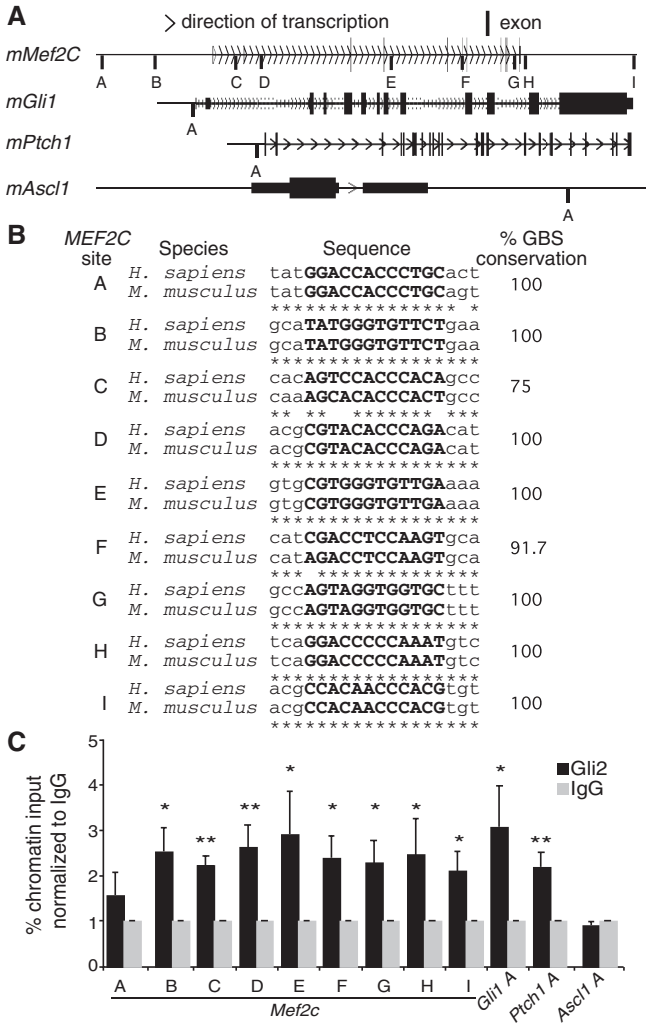

Figure 5. Gli2 associates with *Mef2c* gene elements during cardiomyogenesis *in vitro*. (**A**) Custom tracks of murine *Mef2c*, *Gli1*, *Ptch1* and *Ascl1* genes using UCSC genome browser (http://genome.ucsc.edu). Letters designate conserved Gli binding sites (GBS), their genomic positions are listed in Table 2. Listed genes (±100 kb) from mouse and human genomes were searched for conserved theoretical GBS as described in ref. (61); (**B**) comparison of mouse and human sequences of *Mef2c* A–I sites from (A). The sequence of the Gli2 binding site is marked in bold. (**C**) ChIP analysis of Gli2-bound *Mef2c*, *Gli1*, *Ptch1* and *Ascl1* genes on Day 4 of P19[Gli2] cellular differentiation in the presence of 1% DMSO. Black bars designate genomic regions immunoprecipitated with Gli2-specific antibodies, and grey bars designate genomic regions precipitated with IgG-non-specific antibodies. *Gli1* and *Ptch1* promoters served as positive controls, *Ascl1* gene element served as a negative control. Percent chromatin input was calculated using QPCR analysis and primers listed in Table 2. Error bars represent ± SEM from three biological replicas ($n = 3$). Statistical significance was determined as described in 'Materials and Methods' section. $^{*}P < 0.05$, $^{**}P < 0.01$.

Pax3 and Myf5 transcripts (data not shown), therefore indicating normal skeletal myogenesis. Gli2 mRNA was downregulated in P19[Nkx-MEF2C/EnR] cells on Day 6 of differentiation (Figure 7C, panel Gli2). The loss of Gli2 appears to be specific for a subset of dominant-negative transcription factors, including Nkx-MEF2C/EnR (Figure 7), which caused inhibition of cardiomyogenesis,

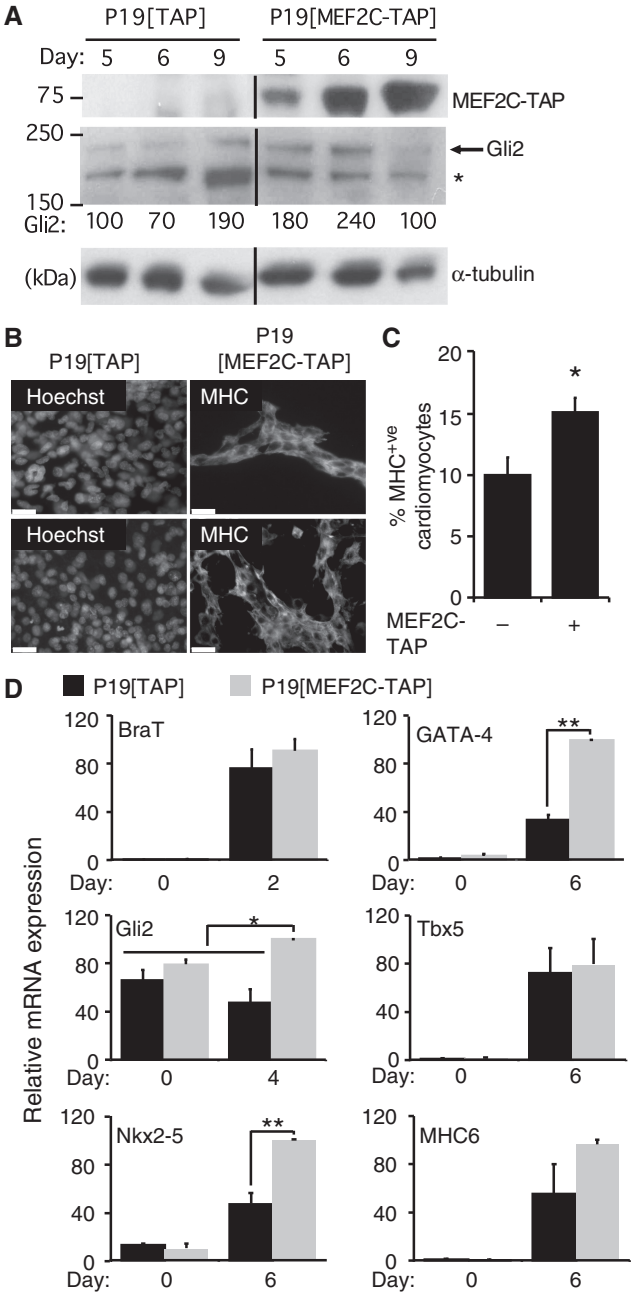

Figure 6. MEF2C upregulates Gli2 expression while enhancing cardiomyogenesis in P19 EC cells. P19[MEF2C-TAP] and P19[TAP] cell lines were differentiated in the presence of 1% DMSO. (**A**) Immunoblot analyses of MEF2C-TAP and Gli2 protein expression in differentiating P19[MEF2C-TAP] and P19[TAP] cells on Days 5, 6 and 9 using Gli2-specific or CBP-specific antibodies. Arrow designates Gli2 protein band, and asterisk denotes non-specific binding of the Gli2 antibodies. α-Tubulin served as a loading control. Lanes were spliced out from the same autoradiogram as designated by vertical lines. Gli2 band densities were measured from one representative experiment using ImageJ program (56) and normalized to α-tubulin. Gli2 band density in P19[TAP] Day 5 sample was set at 100%; (**B**) Day 6 differentiated P19[MEF2C-TAP] and P19[TAP] cultures were reacted with MHC-specific antibodies to detect MHC expression. Nuclei were stained with Hoechst dye. Scale bar is 30 μM; (**C**) MHC-positive cardiomyocytes from (B) were counted in 10 random fields and expressed as percent of the total number of nuclei, $n = 4$. In total, 14 000 cells were counted; (**D**) QPCR analysis of the expression of the genes indicated at the times shown in P19[TAP] (black bars) and P19[MEF2C-TAP] (grey bars) cultures. Error bars represent ± SEM

(continued)

and MyoD/EnR (76), Meox/EnR (47), and ß-catenin/EnR (74), which caused inhibition of skeletal myogenesis (Table 4). In contrast, Gli2 levels were not downregulated in P19 cells expressing Pax/EnR (75) that resulted in the loss of skeletal myogenesis (Table 4). Thus, MEF2C, or genes bound by MEF2C, is essential for maintaining normal Gli2 expression during cardiomyogenesis in P19 EC cells (summarized in Table 4).

MEF2C associates with *Gli2* gene elements during cardiomyogenesis in stem cells

To test if MEF2C can bind *Gli2* gene elements, *in silico* analysis of the *Gli2* gene (± 100 kb) revealed six conserved theoretical MEF2 binding sites (MBS) (*Gli2* A–F, Figure 8A and B, summarized in Table 2) suggesting that Gli2 could be a target of MEF2. ChIP analysis of Day 5 differentiating P19[MEF2C] cells revealed statistically significant enrichment, with a MEF2C antibody, of chromatin fragments corresponding to *Gli2* A–D and F sites, but not to *Gli2* E site (Figure 8C). The *Hdac4* intron region, which is located on the same chromosome as the *Gli2* gene (summarized in Table 2), was not enriched in the ChIP assay with MEF2C antibodies (Figure 8C), therefore serving as a negative control and demonstrating the specificity of ChIP analysis using MEF2C-specific antibodies. The *Gata-4* and *MyoG* promoter regions were used as positive controls (Figure 8C). Therefore, MEF2C is associated with *Gli2* gene elements during cardiomyogenesis in P19 EC cells.

Gli2 and MEF2C factors form a protein complex that can function synergistically

Based on the finding that Gli2 and MEF2C are co-expressed during later stages of cardiomyogenesis in mES and during P19 EC cardiomyogenesis (Figures 1 and 2, respectively) and they regulate each other's expression, as well as have similar abilities to regulate cardiomyogenesis in P19 EC cells (Figures 3 and 6), we hypothesized that these transcription factors may form a protein complex to synergistically regulate the expression of cardiomyogenesis-related genes.

To test this hypothesis, we first explored the ability of Gli2 and MEF2C to synergize in luciferase reporter assays. To this end, we took advantage of an endogenous Nkx2-5 promoter (−3059 to +223 nt relative to Nkx2-5 transcriptional start site), which was shown to drive gene expression in the cardiac crescent at E7.25, as well as outflow tract and right ventricle at E10.5, and require combinatorial function of multiple regulatory factors (59). This Nkx2-5 promoter contained 3XGli, 3XMEF2, 6XGATA-4, 3XNkx and 1XTbx5 binding sites and was

Figure 6. Continued
from two biological replicas of two clonal populations ($n = 4$). Statistical significance using ANOVA test was determined between groups of P19[TAP] and P19[MEF2C-TAP] samples analysed on the same day. For Gli2 expression, ANOVA followed by post hoc Tukey HSD test was performed to determine statistically significant differences between P19[TAP] and P19[MEF2C-TAP] samples on all days analysed. $*P < 0.05$ and $**P < 0.01$. Primers are listed in Table 1.

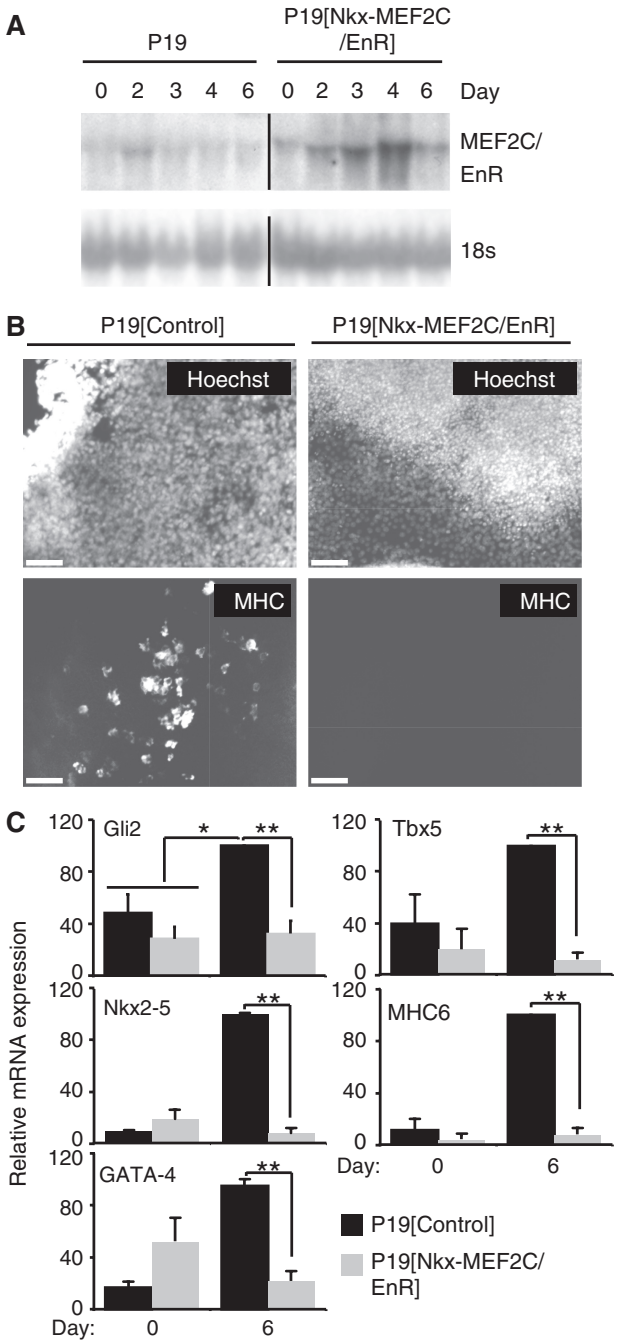

Figure 7. Expression of Nkx-MEF2C/EnR downregulates Gli2 expression while inhibiting cardiomyogenesis in P19 EC cells. P19[Control] and P19[Nkx-MEF2C/EnR] cell lines were differentiated in the presence of 1% DMSO. (**A**) Northern blot analysis of the expression of MEF2C/EnR mRNA in P19 and P19[Nkx-MEF2C/EnR] cells on Days 0 and 2–6. Here, 18 s served as a loading control. Lanes were spliced out from the same autoradiogram as designated by vertical lines. (**B**) Antigenic analysis of P19 and P19[Nkx-MEF2C/EnR] using MHC-specific antibodies on Day 6 of DMSO-induced differentiation. Nuclei were stained with Hoechst dye. Scale bar is 60 µM. (**C**) QPCR analysis of the expression of Nkx2-5, GATA-4, Tbx5, MHC6 and Gli2 mRNA in differentiated P19[Control] and P19[Nkx-MEF2C/EnR] cells on Days 0 and 6. Error bars represent ± SEM from two biological replicas of two clonal populations ($n = 4$). Statistical significance using ANOVA test was determined between groups of P19 and P19[Nkx-MEF2C/EnR] samples analysed on the same day. For Gli2 expression, ANOVA followed by post hoc Tukey HSD test was performed to determine statistically significant differences between P19 and P19[Nkx-MEF2C/EnR] samples on all days analysed. $*P < 0.05$, $**P < 0.01$. Primers are listed in Table 1.

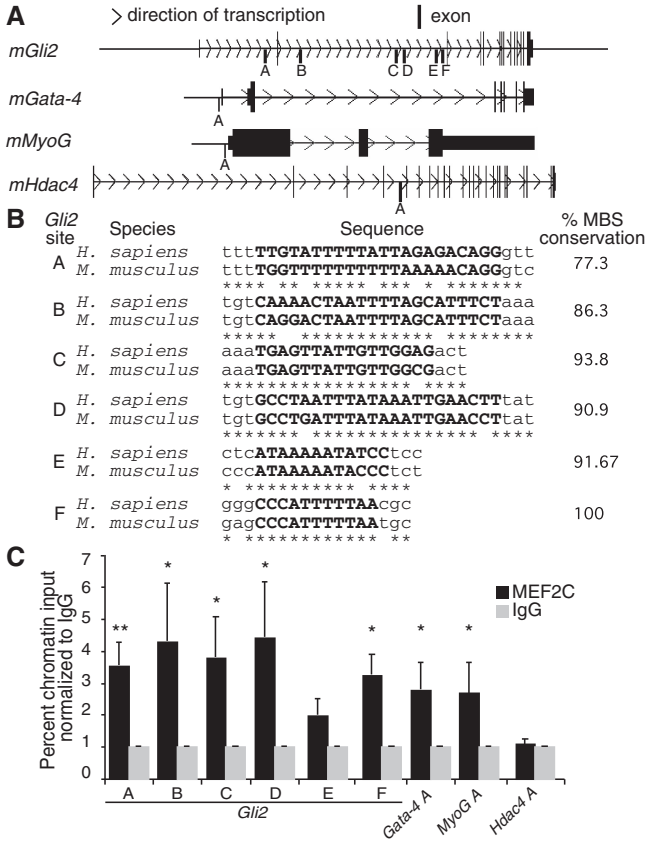

Figure 8. MEF2C associates with *Gli2* gene elements during cardiomyogenesis *in vitro*. P19[TAP] and P19[MEF2C-TAP] cell lines were differentiated in the presence of 1% DMSO. (**A**) Custom tracks of murine *Gli2*, *Gata-4*, *MyoG* and *Hdac4* genes using UCSC genome browser (http://genome.ucsc.edu). Letters designate conserved MEF2 binding sites (MBS), their genomic positions are listed in Table 2. Listed genes (±100 kb) from mouse and human genomes were searched for conserved theoretical MBS as described in ref. (61); (**B**) comparison of mouse and human sequences of *Gli2* A–F sites from (A). The sequence of the MBS is marked in bold. (**C**) ChIP analysis of MEF2C-bound *Gli2*, *Gata-4*, *MyoG* and *Hdac4* genes during P19[MEF2C] cellular differentiation. Black bars designate genomic regions immunoprecipitated with MEF2C-specific antibodies, and grey bars designate genomic regions precipitated with IgG-non-specific antibodies. *Gata-4* and *MyoG* promoters served as positive controls, *Hdac4* gene element served as a negative control. Percent chromatin input was calculated using QPCR analysis and primers are listed in Table 2. Error bars represent ±SEM from three biological replicas ($n = 3$). Statistical significance was determined as described in 'Materials and Methods' section. $^{*}P < 0.05$, $^{**}P < 0.01$.

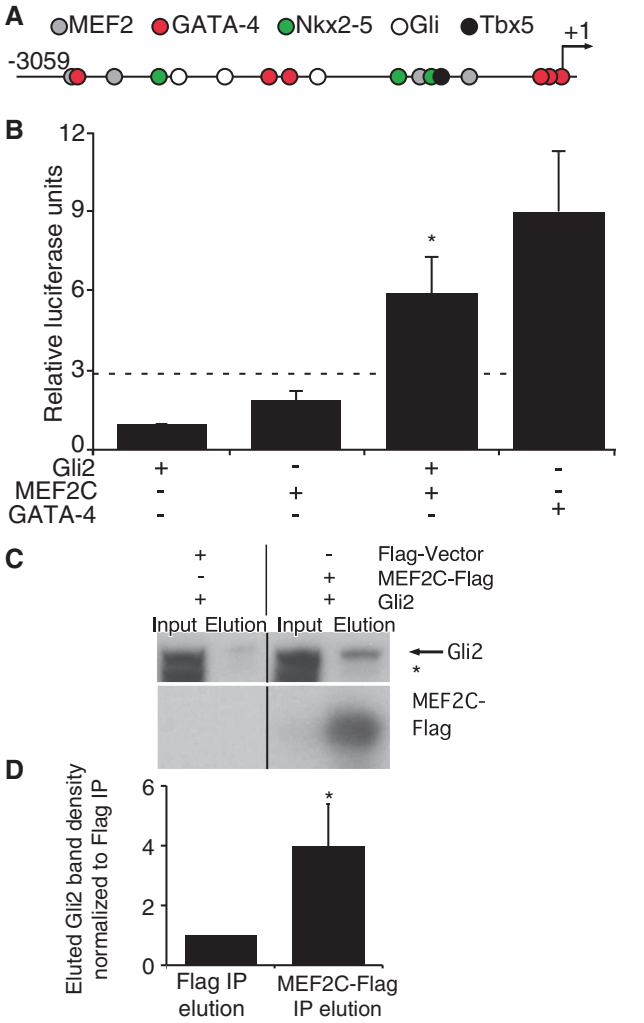

Figure 9. Gli2 and MEF2C form a protein complex and synergize on the Nkx2-5 promoter. (**A**) Schematic representation of Nkx2-5-luc reporter construct. Circles designate Gli (white), MEF2 (grey), Nkx (green), GATA-4 (red) and Tbx5 (black) binding sites; +1 designates transcriptional start site (TSS); −3059 designates the beginning of the Nkx2-5 promoter relative to (TSS); (**B**) Gli2 and MEF2C were transfected alone or together with or without Nkx2-5-luc in P19 cells. Cells transfected with GATA-4 served as a positive control. Error bars represent ±SEM from 10 biological replicas ($n = 10$). $^{*}P < 0.05$. The dashed line represents the value at which Gli2 and MEF2C function additively. Transfection efficiency was monitored by assaying activity of co-transfected Renilla luciferase. Synergy and statistical significance was calculated as described in 'Materials and Methods' section. The average activation of Nkx2-5-luc by Gli2 was 2.3 ± 0.4 (data not shown) and was normalized to 1; (**C**) Gli2 was co-immunoprecipitated with MEF2C-Flag but not with Flag-vector when transfected in HEK-293 cells. Transfection efficiency was monitored by assaying autofluorescence of co-transfected GFP. Arrow designates Gli2 protein band, and asterisk denotes non-specific binding of the Gli2 antibodies. Lanes were spliced out from the same autoradiogram as designated by vertical lines. (**D**) Quantification of Gli2 band density from elution fractions in (C) using ImageJ program. Error bars represent ±SEM from three biological replicas ($n = 3$), $^{*}P < 0.05$.

fused to the luciferase gene (Nkx2-5-luc) (59) (Figure 9A). When Gli2 and MEF2C were co-transfected together, they synergistically activated the Nkx2-5 promoter up to 6 ± 2-fold as compared with the theoretical additive value of 3 ± 0.3-fold change (Figure 9B, dashed line). The activation of the Nkx2-5 promoter by Gli2 and MEF2C together was similar to that of GATA-4 alone (Figure 9B). When Gli2 and MEF2C were co-transfected with luciferase reporters containing either 5xGli or 5xMEF2 binding sites alone, no synergy or additive effect was observed (data not shown). Therefore, Gli2 and MEF2C synergistically activate the Nkx2-5 promoter.

To test if Gli2 and MEF2C formed a protein complex, we co-transfected Gli2 and MEF2C-Flag or Flag-vector into HEK-293 cells. Gli2 co-immunoprecipitated with MEF2C-Flag, but not with the Flag-tag alone

(Figure 9C). Analysis of autofluorescence of co-transfected GFP was performed to ensure that all samples were transfected with equal efficiency. Quantitative analysis of bands corresponding to Gli2 protein revealed a 4 ± 1-fold higher amount of Gli2 co-immunoprecipitated with MEF2C-Flag when compared with co-IP with Flag-vector (Figure 9D). Therefore, Gli2 and MEF2C proteins physically associate and synergistically activate transcription.

DISCUSSION

We have shown that Gli2 and MEF2C are associated with each other's gene elements and are able to regulate each other's expression during cardiomyogenesis in P19 EC cells. Further, Gli2 and MEF2C form a protein complex capable of synergistically activating gene promoters that participate in cardiomyogenesis. Thus, we propose a model similar to that for MEF2 and myogenic regulatory factors (MRFs) [reviewed in ref. (15)], where Gli2 and MEF2C transcription factors induce and maintain each other's expression, as well as form a protein complex that synergizes on promoters containing both Gli and MEF2 binding elements during cardiomyogenesis (Figure 10). It is likely that other transcription factors participate in the Gli2–MEF2C protein complex, designated as '?'.

Our results obtained *in vitro* provide added mechanistic insight into the roles of Gli2 and MEF2C in cardiomyogenesis. Whereas only cardiac outflow tract anomalies were detected in the developing hearts of $Gli2^{-/-}Gli3^{+/-}$ mice (6,14), $MEF2C^{-/-}$ mice had heart looping defects along with gross abnormalities in the right ventricle, as well as in the outflow tract (19,20). This suggests that Gli2 and MEF2C may function co-operatively during cardiac outflow formation. Our studies are consistent with an overlapping pattern of defects that could be explained by Gli2 and MEF2C having both shared and distinct subsets of targets, likely dependent upon the unique protein complexes formed in each case.

The results from this study suggest that both Gli2 and MEF2C may be active at the cardiac muscle progenitor stage. This is supported by the embryonic expression patterns of MEF2C (starting from E7.5) (16,17) and Gli1 (E7.0–8.0) (3,10), which are both expressed after mesodermal markers BraT (E6.5) and MESP1 (E6.5), and concomitantly with the cardiac progenitor marker Nkx2-5 (E7.0) [reviewed in ref. (87)]. Although the expression of Gli2 resulted in downregulated expression of BraT, the decrease was minimal (15 ± 4%) in comparison with the upregulation of expression of other factors (Figure 3D). Furthermore, overexpression of MEF2C, Nkx-MEF2C/EnR and Gli/EnR did not affect the expression of BraT in P19 EC cellular differentiation [refs (21,45,47) and Figure 6D], while affecting the expression of cardiac muscle progenitor markers Nkx2-5 and GATA-4 [(21,41,45) and Figures 4C, 6D and 7C].

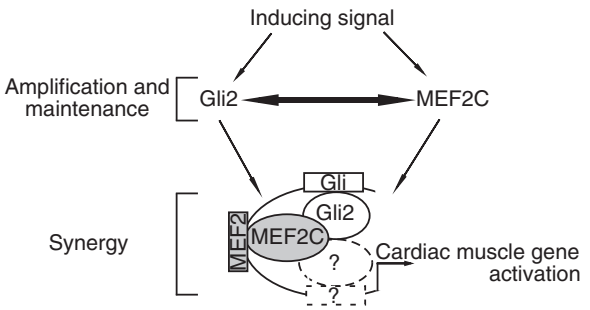

Figure 10. Gli2 and MEF2C interact during cardiomyogenesis *in vitro*. We propose a model in which Gli2 and MEF2C induce each other's expression and bind each other's gene elements (designated by thick arrow), as well as form a protein complex on gene promoters capable of synergistically activating their expression. Other protein(s) participating in the Gli2/MEF2C protein complex are designated by '?'.

The temporal patterns of MEF2C and Gli2 expression we identified in both P19 EC and mES cells are consistent with previous reports. MEF2C mRNA is upregulated during cardiomyogenesis in mES cells by Day 6, after expression of mesodermal markers BraT and Mesp1/2 (72) and in P19 EC cells from Days 6–7 (27), similar to our findings (Figures 1 and 2). Much less information is available about the expression of Gli transcription factors during ES myogenesis. It is known that Shh signalling members are expressed in undifferentiated hES cells (88), as well as in cardiomyocytes derived from P19 EC (41,42), P19CL6 (43) and mES cells stably expressing neomycin-resistance gene under the regulation of cardiac α-MHC promoter (23). A further complication is that Gli2 is expressed in numerous lineages, including brain, bone, cartilage, muscle, lung and pancreas [reviewed in ref. (89)]. In addition, Gli2 might be involved in maintaining stem cell pluripotency in ES cells as it was shown to directly regulate expression of the pluripotency markers Sox2 (90) and Nanog (91). Thus, it is possible that a high level of Gli2 expression is necessary to maintain the pluripotent state of ES cells, and lower level of Gli2 expression is sufficient to support mES differentiation. This phenomenon has been shown previously for Oct-4 and Sox2, which play roles in maintaining pluripotency (66,92), as well as in directing early stages of ES cell differentiation (67,93). Finally, the primary effect of the Hedgehog (Hh) signalling is the activation of Gli2 protein function, as opposed to the upregulation of Gli2 mRNA or protein expression (94,95). The elevated expression of Ptch1, marker of active Hh signalling (96), during Days 6–9 of mES differentiation (Figure 1D), suggests that the Hh signalling pathway is active when MEF2C is expressed in differentiating mES cells (Figure 1D).

In comparison with mES cells (77,97), DMSO-treated P19 EC cells differentiate into only a limited number of mesodermal and endodermal lineages (27,30–34). In this system, Gli2 expression was upregulated during cardiomyogenesis from Days 5–6 (Figure 2D), in agreement with previous studies (41,42). Furthermore, Gli2 was significantly upregulated in the same temporal pattern as MEF2C (Figure 2D). In summary, P19 EC cells provide a good model system for examining the functional interaction between Gli2 and MEF2C.

It was previously demonstrated that Gli2 induced the expression of MEF2C and cardiomyogenesis in P19 EC

cells in the absence of DMSO (41). Recently, it was shown that the activation of the Shh signalling pathway upregulated MEF2C mRNA transcript levels in the second heart field *in vivo* after chick embryos were treated with Shh signalling pathway activator, SAG agonist, at HH14 (98). *Drosophila* embryos expressing mutant loss-of-function MEF2 protein showed downregulated expression of Ci (Cubitus Interruptus, a single *Drosophila* homolog of vertebrate Gli transcription factors) (99). Our results support and extend previous results by showing that Gli2 and MEF2C can upregulate each other's expression while enhancing DMSO-induced cardiomyogenesis in P19 EC cells, suggesting the possibility that they function in a regulatory loop.

Gli2 and MEF2C enhanced each other's mRNA expression on Day 4 of differentiation, and not in undifferentiated cells (Day 0). It was previously shown that MyoD, a master-regulator of skeletal myogenesis capable of converting fibroblasts into skeletal myocytes (100), induced skeletal myogenesis in P19 EC cells only upon cellular aggregation (101,102). Indeed, all of the muscle transcription factors studied to date in P19 EC cells required cellular aggregation to be functional (21,40,45–47,50,52,74–76,78,101–103,114). It is therefore not surprising that the expression levels of Gli2 and MEF2C were not affected in undifferentiated (Day 0) P19 stable cell lines.

The expression of dominant-negative Gli2 resulted in downregulation of MEF2C expression and cardiomyogenesis. To our knowledge, this is the first indication that the expression of Gli/EnR results in impaired cardiomyogenesis in P19 EC cells. Previous reports showed that Shh signalling is not essential for cardiomyogenesis during embryogenesis (3,4) or in P19 EC cells (42), although a reduction or delay of cardiomyogenesis was observed. However, treatment of a cardiac lineage-restricted subline of P19 cells, P19CL6 cells, with the Shh signalling inhibitor cyclopamine blocked their differentiation into beating cardiac myocytes (43). The difference in the latter results may be due to a lack of compensatory signalling molecules, derived from other lineages, implicated in activating Gli factors, such as TGFβ (104), Fgf (105) and Wnt (106). Finally, Zic factors have also been shown to bind genomic Gli binding sites and to modulate the transcriptional activity of Gli transcription factors (107). Our use of a dominant-negative approach would override compensatory activating signals (47,55), showing a role for Gli2 function during cardiomyogenesis.

While ubiquitously expressed Gli2 and MEF2C each enhanced cardiomyogenesis (Figures 3 and 6), and ubiquitously expressed Gli/EnR impaired cardiomyogenesis (Figure 4), surprisingly *pgk*-driven MEF/EnR enhanced cardiomyogenesis (46) and skeletal myogenesis (Karamboulas and Skerjanc, unpublished data). This is likely due to the dual nature of MEF2 factors, which have the ability to recruit HDAC4/5 to genes, inhibiting transcription (108), as well as recruiting histone acetyltransferases, activating transcription (108). A repressive role for Gli2 in regulating entry into various lineages was not observed, since the expression of Gli/EnR under the *pgk* promoter resulted in abolished skeletal myogenesis (47) and attenuated levels of neurogenesis and gliogenesis (55) at a specific stage of each respective differentiation program (47,55). Therefore, expression of Gli2/EnR under a general promoter such as *pgk*, impaired the formation of different stem cell differentiation pathways, including cardiomyogenesis, at specific stages.

While overexpression of MEF2C-TAP upregulated transcript levels of Gli2, Nkx2-5 and GATA-4, it did not affect Tbx5 mRNA expression. This correlates with previous studies, where knockdown of MEF2C using morpholinos disrupted zebrafish heart tube looping, but did not affect Tbx5 expression (109). It is possible that other MEF2 family proteins were able to rescue the expression of Tbx5 in zebrafish (109). Genetic redundancy of MEF2C family members is supported by our finding that the expression of Tbx5, Gli2 and cardiac muscle progenitor markers was drastically reduced in the presence of dominant-negative Nkx-MEF2C/EnR *in vitro*, and the loss of heart formation *in vivo* (21). It is likely that the Nkx2-5 enhancer driving the expression of MEF2C/EnR can be regulated by Gli2 and the previously described regulatory loop between MEF2C, GATA-4 and Nkx2-5 (21,40,45,78). Thus, as Nkx2-5 is expressed during formation of cardiac muscle progenitors, the overexpression of Nkx-MEF2C/EnR will inhibit the function of endogenous MEF2C and Gli2, as well as other cardiogenic factors, resulting in the loss of cardiomyogenesis. This is supported by the fact that both endogenous Gli2 and MEF2C were downregulated, but not abolished, by Day 6 in P19[Nkx-MEF2C/EnR] cells, whereas the expression of Nkx-MEF2C/EnR was reduced [ref. (21) and Figure 7].

We report for the first time that Gli2 and MEF2C associate with each other's gene elements. Although existing literature supports identification of Gli2 as a target of MEF2C by demonstrating that the *Drosophila* MEF2 protein directly bound gene elements of Ci (a *Drosophila* homolog of vertebrate Gli transcription factors) (99), MEF2C was not previously reported to be a target of Gli3 in murine developing limb in a genome-wide ChIP-on-chip analysis (110). It is possible that MEF2C is a target of the Gli transcription factors at an earlier time-point than the time-point analysed in the study (E11.5) (110). Members of the Shh signalling pathway are expressed starting from E8.0 in murine paraxial mesoderm (81) and MEF2C is the first MEF2 family factor to be expressed in somites starting from E8.5–9.0 (16). Finally, it is possible that MEF2C is a target of Gli2 and not Gli3, during cardiomyogenesis.

Notably, the majority of the Gli2-bound sites are located in the intron regions of the *Mef2c* gene. It was previously shown that there are multiple promoter and enhancer regulatory elements within the *Mef2c* gene introns (17,111,112). Of those known regulatory elements in the *Mef2c* gene, the *Mef2c D* site, which was bound by Gli2 in this study, is located ∼+500 bp relative to the 3′-end of the reported cardiac promoter (17). Thus, it is possible that other *Mef2c* gene elements bound by Gli2 are located within novel regulatory regions, however, their identification is outside the scope of this study.

Much like the *Mef2c* gene sites bound by the Gli2 protein, *Gli2* sites bound by the MEF2C protein are located in the intron regions of the *Gli2* gene. Although regulatory elements in the *Gli2* gene have not yet been reported, it is possible that its introns contain novel uncharacterized regulatory regions. For example, the *Gli2 B* site that was bound by MEF2C in this study, is part of the predicted genomic enhancer, which is well conserved between human, mouse, chicken, frog and fugu genomes [ref. (113), element hs1790]. Although this region was not found to have any enhancer activity at E11.5 when transfected into mouse embryos in a reporter cassette driving β-gal expression [ref. (113), element hs1790], it is possible that it can act as an enhancer at an earlier or later time point in development.

Both Gli2 and MEF2C are capable of enhancing the development of cardiac muscle through upregulation of the Nkx2-5, GATA-4 and BMP-4 regulatory loop [this study and refs (41,45)], skeletal muscle via upregulation of MRFs (47,48) and neurons through enhancement of Ascl1/Mash1 expression (55,114) in pluripotent P19 EC cells. The ability of Gli2 and MEF2C to regulate a similar subset of differentiation pathways in pluripotent P19 EC cells, led us to hypothesize that Gli2 and MEF2C could function together. We showed that Gli2 and MEF2C form a protein complex that functions synergistically on the Nkx2-5 promoter. MEF2 proteins are known to form synergistic protein complexes with cardiac muscle factors such as Hand1 (115) and GATA-4 (116). More recently, MEF2C, together with GATA-4 and Tbx5, was shown to convert mouse fibroblasts into cardiac myocytes (117). Furthermore, our findings are consistent with Pitx2, which is a homeodomain transcription factor involved in heart development, and MEF2 protein complex studies, where both MEF2 and Pitx2 DNA binding sites were necessary for the synergistic action of the protein complex (118).

In silico analysis of the mouse genome identified 957 genes containing both Gli and MEF2 conserved DNA binding clusters (Supplementary Table S1). Functional annotation analysis of these potential targets revealed a number of categories enriched among Gli and MEF clusters containing genes, such as cell differentiation, regulation of gene expression, chromatin organization, as well as development of nervous system, heart, the skeletal system and muscle organ (Table 3). While Nkx2-5 was not identified as a target gene for Gli2 and MEF2C, probably due to the presence of non-conserved Gli and MEF2 binding elements and/or due to stringent restrictions used in the screening process, MEF2C was identified as one of the potential target genes for both Gli and MEF2 transcription factors (Supplementary Table S1 and Table 3). The identification of numerous potential Gli and MEF2 targets regulating various lineages implies that the Gli2/MEF2C interactions identified here may be applicable to other lineages and require further study.

In summary, we propose a novel mechanistic model, in which Gli2 and MEF2C transcription factors induce and maintain each other's expression, as well as form a protein complex capable of synergizing on gene promoters containing both Gli and MEF2 binding elements during cardiomyogenesis *in vitro* (Figure 10). This is the first evidence that the Shh signalling pathway is directly linked to the function of MEF2C protein. Our findings are similar to the MEF2 and MRF interaction model [reviewed in ref. (15)]. The Gli2/MEF2C protein complex may function during the induction of several lineages, including cardiac and skeletal muscle, as well as neurons. This is supported by the identification of numerous putative targets for both Gli2 and MEF2C, which are enriched in neurogenesis, as well as skeletal muscle and heart developmental processes (Table 3). Understanding the complex network of transcription factors that regulates lineage determination during stem cell differentiation is important for potential future cell therapies.

SUPPLEMENTARY DATA

Supplementary Data are available at NAR Online: Supplementary Table 1.

ACKNOWLEDGEMENTS

The authors would like to thank J. Fair and D. Ebadi for technical assistance, Dr Hui for providing Gli2 specific antibodies, Dr Sasaki for Gli2 expression plasmid and Gli-responsive reporter construct, Dr Yutzey for Nkx2-5-luc, Dr Nemer for GATA-4 expressing plasmid, Dr Wallace for eye total protein extracts from $Gli2^{+/-}$ and $Gli2^{-/-}$ mice, Dr Wallace. Dr Brand and Dr Blais for helpful discussions and Dr Ryan, V. Mehta and D. Ebadi for critical reading of the manuscript. A.V. carried out mES, parental and stable P19 EC differentiation, IF, QPCR analysis, ChIP assay with Gli2 antibodies, IP from HEK-293 cells, bioinformatics analysis and manuscript writing. A.M. created and differentiated P19[TAP] and P19[MEF2C-TAP] stable cell lines and carried out ChIP assay with MEF2C antibodies. A.F. participated in ChIP assay with Gli2 antibodies. M.S. participated in differentiation and QPCR analysis of mES cells. C.K. differentiated P19[Nkx-MEF2C/EnR] cells, carried out northern blot and IF analysis of this cell line. I.S.S. conceived the study and participated in its design and coordination and helped to draft the manuscript. All authors read and approved the final manuscript.

FUNDING

Canadian Institutes of Health Research (MOP-53277 to I.S.S.); Heart and Stroke Foundation of Canada Doctoral Research Award (to A.V.); Ontario Graduate Scholarship (to A.V. and M.S.). Funding for open access charge: Canadian Institutes of Health Research (MOP-53277 to I.S.S.)

Conflict of interest statement. None declared.

REFERENCES

1. Buckingham,M., Meilhac,S. and Zaffran,S. (2005) Building the mammalian heart from two sources of myocardial cells. *Nat. Rev. Genet.*, **6**, 826–835.
2. Black,B.L. (2007) Transcriptional pathways in second heart field development. *Semin. Cell Dev. Biol.*, **18**, 67–76.
3. Thomas,N.A., Koudijs,M., van Eeden,F.J., Joyner,A.L. and Yelon,D. (2008) Hedgehog signaling plays a cell-autonomous role in maximizing cardiac developmental potential. *Development*, **135**, 3789–3799.
4. Zhang,X.M., Ramalho-Santos,M. and McMahon,A.P. (2001) Smoothened mutants reveal redundant roles for Shh and Ihh signaling including regulation of L/R symmetry by the mouse node. *Cell*, **106**, 781–792.
5. Washington Smoak,I., Byrd,N.A., Abu-Issa,R., Goddeeris,M.M., Anderson,R., Morris,J., Yamamura,K., Klingensmith,J. and Meyers,E.N. (2005) Sonic hedgehog is required for cardiac outflow tract and neural crest cell development. *Dev. Biol.*, **283**, 357–372.
6. Kim,P.C., Mo,R. and Hui Cc,C. (2001) Murine models of VACTERL syndrome: role of sonic hedgehog signaling pathway. *J. Pediatr. Surg.*, **36**, 381–384.
7. Dyer,L.A. and Kirby,M.L. (2009) Sonic hedgehog maintains proliferation in secondary heart field progenitors and is required for normal arterial pole formation. *Dev. Biol.*, **330**, 305–317.
8. Goddeeris,M.M., Schwartz,R., Klingensmith,J. and Meyers,E.N. (2007) Independent requirements for Hedgehog signaling by both the anterior heart field and neural crest cells for outflow tract development. *Development*, **134**, 1593–1604.
9. Goddeeris,M.M., Rho,S., Petiet,A., Davenport,C.L., Johnson,G.A., Meyers,E.N. and Klingensmith,J. (2008) Intracardiac septation requires hedgehog-dependent cellular contributions from outside the heart. *Development*, **135**, 1887–1895.
10. Hoffmann,A.D., Peterson,M.A., Friedland-Little,J.M., Anderson,S.A. and Moskowitz,I.P. (2009) Sonic hedgehog is required in pulmonary endoderm for atrial septation. *Development*, **136**, 1761–1770.
11. Riobo,N.A. and Manning,D.R. (2007) Pathways of signal transduction employed by vertebrate Hedgehogs. *Biochem. J.*, **403**, 369–379.
12. Ruiz,I.A.A., Palma,V. and Dahmane,N. (2002) Hedgehog-Gli signalling and the growth of the brain. *Nat. Rev. Neurosci.*, **3**, 24–33.
13. Kinzler,K.W. and Vogelstein,B. (1990) The GLI gene encodes a nuclear protein which binds specific sequences in the human genome. *Mol. Cell Biol.*, **10**, 634–642.
14. Kim,J., Kim,P. and Hui,C.C. (2001) The VACTERL association: lessons from the Sonic hedgehog pathway. *Clin. Genet.*, **59**, 306–315.
15. Potthoff,M.J. and Olson,E.N. (2007) MEF2: a central regulator of diverse developmental programs. *Development*, **134**, 4131–4140.
16. Edmondson,D.G., Lyons,G.E., Martin,J.F. and Olson,E.N. (1994) Mef2 gene expression marks the cardiac and skeletal muscle lineages during mouse embryogenesis. *Development*, **120**, 1251–1263.
17. Dodou,E., Verzi,M.P., Anderson,J.P., Xu,S.M. and Black,B.L. (2004) Mef2c is a direct transcriptional target of ISL1 and GATA factors in the anterior heart field during mouse embryonic development. *Development*, **131**, 3931–3942.
18. Lilly,B., Zhao,B., Ranganayakulu,G., Paterson,B.M., Schulz,R.A. and Olson,E.N. (1995) Requirement of MADS domain transcription factor D-MEF2 for muscle formation in Drosophila. *Science*, **267**, 688–693.
19. Lin,Q., Schwarz,J., Bucana,C. and Olson,E.N. (1997) Control of mouse cardiac morphogenesis and myogenesis by transcription factor MEF2C. *Science*, **276**, 1404–1407.
20. Vong,L.H., Ragusa,M.J. and Schwarz,J.J. (2005) Generation of conditional Mef2cloxP/loxP mice for temporal- and tissue-specific analyses. *Genesis*, **43**, 43–48.
21. Karamboulas,C., Dakubo,G.D., Liu,J., De Repentigny,Y., Yutzey,K., Wallace,V.A., Kothary,R. and Skerjanc,I.S. (2006) Disruption of MEF2 activity in cardiomyoblasts inhibits cardiomyogenesis. *J. Cell. Sci.*, **119**, 4315–4321.
22. Chen,K., Wu,L. and Wang,Z.Z. (2008) Extrinsic regulation of cardiomyocyte differentiation of embryonic stem cells. *J. Cell. Biochem.*, **104**, 119–128.
23. Seewald,M.J., Ellinghaus,P., Kassner,A., Stork,I., Barg,M., Niebrugge,S., Golz,S., Summer,H., Zweigerdt,R., Schrader,E.M. *et al.* (2009) Genomic profiling of developing cardiomyocytes from recombinant murine embryonic stem cells reveals regulation of transcription factor clusters. *Physiol. Genomics*, **38**, 7–15.
24. Synnergren,J., Akesson,K., Dahlenborg,K., Vidarsson,H., Ameen,C., Steel,D., Lindahl,A., Olsson,B. and Sartipy,P. (2008) Molecular signature of cardiomyocyte clusters derived from human embryonic stem cells. *Stem Cells*, **26**, 1831–1840.
25. Al Madhoun,A.S., Mehta,V., Li,G., Figeys,D., Wiper-Bergeron,N. and Skerjanc,I.S. (2011) Skeletal myosin light chain kinase regulates skeletal myogenesis by phosphorylation of MEF2C. *EMBO J.*, **30**, 2477–2489.
26. McBurney,M.W. and Rogers,B.J. (1982) Isolation of male embryonal carcinoma cells and their chromosome replication patterns. *Dev. Biol.*, **89**, 503–508.
27. Skerjanc,I.S. (1999) Cardiac and skeletal muscle development in P19 embryonal carcinoma cells. *Trends Cardiovasc. Med.*, **9**, 139–143.
28. van der Heyden,M.A. and Defize,L.H. (2003) Twenty one years of P19 cells: what an embryonal carcinoma cell line taught us about cardiomyocyte differentiation. *Cardiovasc. Res.*, **58**, 292–302.
29. Astigiano,S., Damonte,P., Fossati,S., Boni,L. and Barbieri,O. (2005) Fate of embryonal carcinoma cells injected into postimplantation mouse embryos. *Differentiation*, **73**, 484–490.
30. McBurney,M.W., Jones-Villeneuve,E.M., Edwards,M.K. and Anderson,P.J. (1982) Control of muscle and neuronal differentiation in a cultured embryonal carcinoma cell line. *Nature*, **299**, 165–167.
31. Edwards,M.K., Harris,J.F. and McBurney,M.W. (1983) Induced muscle differentiation in an embryonal carcinoma cell line. *Mol. Cell Biol.*, **3**, 2280–2286.
32. McBurney,M.W. (1993) P19 embryonal carcinoma cells. *Int. J. Dev. Biol.*, **37**, 135–140.
33. Rudnicki,M.A. and McBurney,M.W. (1987) Cell culture methods and induction of differentiation of embryonal carcinoma cell lines. In: Robertson,E.J. (ed.), *Teratocarcinomas and Embryonic Stem Cells. A Practical Approach*. IRL Press, Oxford, pp. 19–49.
34. Smith,S.C., Reuhl,K.R., Craig,J. and McBurney,M.W. (1987) The role of aggregation in embryonal carcinoma cell differentiation. *J. Cell. Physiol.*, **131**, 74–84.
35. Kennedy,K.A., Porter,T., Mehta,V., Ryan,S.D., Price,F., Peshdary,V., Karamboulas,C., Savage,J., Drysdale,T.A., Li,S.C. *et al.* (2009) Retinoic acid enhances skeletal muscle progenitor formation and bypasses inhibition by bone morphogenetic protein 4 but not dominant negative beta-catenin. *BMC Biol.*, **7**, 67.
36. Ryan,T., Liu,J., Chu,A., Wang,L., Blais,A. and Skerjanc,I.S. (2011) Retinoic acid enhances skeletal myogenesis in human embryonic stem cells by expanding the premyogenic progenitor population. *Stem Cell Rev.* (doi: 10.1007/s12015-011-9284-0, epub ahead of print).
37. Vermot,J. and Pourquie,O. (2005) Retinoic acid coordinates somitogenesis and left-right patterning in vertebrate embryos. *Nature*, **435**, 215–220.
38. Bang,A.G., Papalopulu,N., Kintner,C. and Goulding,M.D. (1997) Expression of Pax-3 is initiated in the early neural plate by posteriorizing signals produced by the organizer and by posterior non-axial mesoderm. *Development*, **124**, 2075–2085.
39. Fu,Y., Yan,W., Mohun,T.J. and Evans,S.M. (1998) Vertebrate tinman homologues XNkx2-3 and XNkx2-5 are required for heart formation in a functionally redundant manner. *Development*, **125**, 4439–4449.
40. Jamali,M., Rogerson,P.J., Wilton,S. and Skerjanc,I.S. (2001) Nkx2-5 activity is essential for cardiomyogenesis. *J. Biol. Chem.*, **276**, 42252–42258.
41. Gianakopoulos,P.J. and Skerjanc,I.S. (2005) Hedgehog signaling induces cardiomyogenesis in P19 cells. *J. Biol. Chem.*, **280**, 21022–21028.

42. Gianakopoulos,P.J. and Skerjanc,I.S. (2009) Cross talk between hedgehog and bone morphogenetic proteins occurs during cardiomyogenesis in P19 cells. *In Vitro Cell. Dev. Biol. Anim.*, **45**, 566–572.
43. Clement,C.A., Kristensen,S.G., Mollgard,K., Pazour,G.J., Yoder,B.K., Larsen,L.A. and Christensen,S.T. (2009) The primary cilium coordinates early cardiogenesis and hedgehog signaling in cardiomyocyte differentiation. *J. Cell. Sci.*, **122**, 3070–3082.
44. Peng,C.F., Wei,Y., Levsky,J.M., McDonald,T.V., Childs,G. and Kitsis,R.N. (2002) Microarray analysis of global changes in gene expression during cardiac myocyte differentiation. *Physiol. Genomics*, **9**, 145–155.
45. Skerjanc,I.S., Petropoulos,H., Ridgeway,A.G. and Wilton,S. (1998) Myocyte enhancer factor 2C and Nkx2-5 up-regulate each other's expression and initiate cardiomyogenesis in P19 cells. *J. Biol. Chem.*, **273**, 34904–34910.
46. Karamboulas,C., Swedani,A., Ward,C., Al-Madhoun,A.S., Wilton,S., Boisvenue,S., Ridgeway,A.G. and Skerjanc,I.S. (2006) HDAC activity regulates entry of mesoderm cells into the cardiac muscle lineage. *J. Cell. Sci.*, **119**, 4305–4314.
47. Petropoulos,H., Gianakopoulos,P.J., Ridgeway,A.G. and Skerjanc,I.S. (2004) Disruption of Meox or Gli activity ablates skeletal myogenesis in P19 cells. *J. Biol. Chem.*, **279**, 23874–23881.
48. Ridgeway,A.G., Wilton,S. and Skerjanc,I.S. (2000) Myocyte enhancer factor 2C and myogenin up-regulate each other's expression and induce the development of skeletal muscle in P19 cells. *J. Biol. Chem.*, **275**, 41–46.
49. Mo,R., Freer,A.M., Zinyk,D.L., Crackower,M.A., Michaud,J., Heng,H.H., Chik,K.W., Shi,X.M., Tsui,L.C., Cheng,S.H. *et al.* (1997) Specific and redundant functions of Gli2 and Gli3 zinc finger genes in skeletal patterning and development. *Development*, **124**, 113–123.
50. Ridgeway,A.G., Petropoulos,H., Wilton,S. and Skerjanc,I.S. (2000) Wnt signaling regulates the function of MyoD and myogenin. *J. Biol. Chem.*, **275**, 32398–32405.
51. Savage,J., Voronova,A., Mehta,V., Sendi-Mukasa,F. and Skerjanc,I.S. (2010) Canonical Wnt signaling regulates Foxc1/2 expression in P19 cells. *Differentiation*, **79**, 31–40.
52. Savage,J., Conley,A.J., Blais,A. and Skerjanc,I.S. (2009) SOX15 and SOX7 differentially regulate the myogenic program in P19 cells. *Stem Cells*, **27**, 1231–1243.
53. Livak,K.J. and Schmittgen,T.D. (2001) Analysis of relative gene expression data using real-time quantitative PCR and the 2(-Delta Delta C(T)) method. *Methods*, **25**, 402–408.
54. Hu,M.C., Mo,R., Bhella,S., Wilson,C.W., Chuang,P.T., Hui,C.C. and Rosenblum,N.D. (2006) GLI3-dependent transcriptional repression of Gli1, Gli2 and kidney patterning genes disrupts renal morphogenesis. *Development*, **133**, 569–578.
55. Voronova,A., Fischer,A., Ryan,T., Al Madhoun,A. and Skerjanc,I.S. (2011) Ascl1/Mash1 is a novel target of Gli2 during Gli2-induced neurogenesis in P19 EC cells. *PLoS One*, **6**, e19174.
56. Abràmoff,M.D., Magalhães,P.J. and Ram,S.J. (2004) Image processing with ImageJ. *Biophotonics Int.*, **11**, 36–42.
57. Durocher,D., Charron,F., Warren,R., Schwartz,R.J. and Nemer,M. (1997) The cardiac transcription factors Nkx2-5 and GATA-4 are mutual cofactors. *EMBO J.*, **16**, 5687–5696.
58. Sasaki,H., Hui,C., Nakafuku,M. and Kondoh,H. (1997) A binding site for Gli proteins is essential for HNF-3beta floor plate enhancer activity in transgenics and can respond to Shh in vitro. *Development*, **124**, 1313–1322.
59. Searcy,R.D., Vincent,E.B., Liberatore,C.M. and Yutzey,K.E. (1998) A GATA-dependent nkx-2.5 regulatory element activates early cardiac gene expression in transgenic mice. *Development*, **125**, 4461–4470.
60. Markus,M., Du,Z. and Benezra,R. (2002) Enhancer-specific modulation of E protein activity. *J. Biol. Chem.*, **277**, 6469–6477.
61. Ovcharenko,I., Loots,G.G., Giardine,B.M., Hou,M., Ma,J., Hardison,R.C., Stubbs,L. and Miller,W. (2005) Mulan: multiple-sequence local alignment and visualization for studying function and evolution. *Genome Res.*, **15**, 184–194.
62. Rozen,S. and Skaletsky,H. (2000) Primer3 on the WWW for general users and for biologist programmers. *Methods Mol. Biol.*, **132**, 365–386.
63. Ovcharenko,I. and Nobrega,M.A. (2005) Identifying synonymous regulatory elements in vertebrate genomes. *Nucleic Acids Res.*, **33**, W403–W407.
64. Huang da,W., Sherman,B.T. and Lempicki,R.A. (2009) Systematic and integrative analysis of large gene lists using DAVID bioinformatics resources. *Nat. Protoc.*, **4**, 44–57.
65. Huang da,W., Sherman,B.T. and Lempicki,R.A. (2009) Bioinformatics enrichment tools: paths toward the comprehensive functional analysis of large gene lists. *Nucleic Acids Res.*, **37**, 1–13.
66. Niwa,H., Miyazaki,J. and Smith,A.G. (2000) Quantitative expression of Oct-3/4 defines differentiation, dedifferentiation or self-renewal of ES cells. *Nat. Genet.*, **24**, 372–376.
67. Zeineddine,D., Papadimou,E., Chebli,K., Gineste,M., Liu,J., Grey,C., Thurig,S., Behfar,A., Wallace,V.A., Skerjanc,I.S. *et al.* (2006) Oct-3/4 dose dependently regulates specification of embryonic stem cells toward a cardiac lineage and early heart development. *Dev. Cell*, **11**, 535–546.
68. Stennard,F., Ryan,K. and Gurdon,J.B. (1997) Markers of vertebrate mesoderm induction. *Curr. Opin. Genet. Dev.*, **7**, 620–627.
69. Charron,F. and Nemer,M. (1999) GATA transcription factors and cardiac development. *Semin. Cell Dev. Biol.*, **10**, 85–91.
70. Plageman,T.F. Jr and Yutzey,K.E. (2004) Differential expression and function of Tbx5 and Tbx20 in cardiac development. *J. Biol. Chem.*, **279**, 19026–19034.
71. Lints,T.J., Parsons,L.M., Hartley,L., Lyons,I. and Harvey,R.P. (1993) Nkx-2.5: a novel murine homeobox gene expressed in early heart progenitor cells and their myogenic descendants. *Development*, **119**, 419–431.
72. Bondue,A., Lapouge,G., Paulissen,C., Semeraro,C., Iacovino,M., Kyba,M. and Blanpain,C. (2008) Mesp1 acts as a master regulator of multipotent cardiovascular progenitor specification. *Cell Stem Cell*, **3**, 69–84.
73. Jinzhan,W., Kubota,J., Hirayama,J., Nagai,Y., Nishina,S., Yokoi,T., Asaoka,Y., Seo,J., Shimizu,N., Kajiho,H. *et al.* (2010) p38 mitogen-activated protein kinase controls a switch between cardiomyocyte and neuronal commitment of murine embryonic stem cells by activating MEF2C-dependent BMP2 transcription. *Stem Cells Dev.*, **19**, 1723–1734.
74. Petropoulos,H. and Skerjanc,I.S. (2002) Beta-catenin is essential and sufficient for skeletal myogenesis in P19 cells. *J. Biol. Chem.*, **277**, 15393–15399.
75. Ridgeway,A.G. and Skerjanc,I.S. (2001) Pax3 is essential for skeletal myogenesis and the expression of Six1 and Eya2. *J. Biol. Chem.*, **276**, 19033–19039.
76. Gianakopoulos,P.J., Mehta,V., Voronova,A., Cao,Y., Yao,Z., Coutu,J., Wang,X., Waddington,M.S., Tapscott,S.J. and Skerjanc,I.S. (2011) MyoD directly up-regulates premyogenic mesoderm factors during induction of skeletal myogenesis in stem cells. *J. Biol. Chem.*, **286**, 2517–2525.
77. Williams,R.L., Hilton,D.J., Pease,S., Willson,T.A., Stewart,C.L., Gearing,D.P., Wagner,E.F., Metcalf,D., Nicola,N.A. and Gough,N.M. (1988) Myeloid leukaemia inhibitory factor maintains the developmental potential of embryonic stem cells. *Nature*, **336**, 684–687.
78. Grepin,C., Nemer,G. and Nemer,M. (1997) Enhanced cardiogenesis in embryonic stem cells overexpressing the GATA-4 transcription factor. *Development*, **124**, 2387–2395.
79. Park,H.L., Bai,C., Platt,K.A., Matise,M.P., Beeghly,A., Hui,C.C., Nakashima,M. and Joyner,A.L. (2000) Mouse Gli1 mutants are viable but have defects in SHH signaling in combination with a Gli2 mutation. *Development*, **127**, 1593–1605.
80. Bai,C.B., Stephen,D. and Joyner,A.L. (2004) All mouse ventral spinal cord patterning by hedgehog is Gli dependent and involves an activator function of Gli3. *Dev. Cell*, **6**, 103–115.
81. McDermott,A., Gustafsson,M., Elsam,T., Hui,C.C., Emerson,C.P. Jr and Borycki,A.G. (2005) Gli2 and Gli3 have redundant and context-dependent function in skeletal muscle formation. *Development*, **132**, 345–357.
82. Lipinski,R.J., Gipp,J.J., Zhang,J., Doles,J.D. and Bushman,W. (2006) Unique and complimentary activities of the Gli transcription factors in Hedgehog signaling. *Exp. Cell Res.*, **312**, 1925–1938.

83. Montross,W.T., Ji,H. and McCrea,P.D. (2000) A beta-catenin/engrailed chimera selectively suppresses Wnt signaling. *J. Cell Sci.*, **113**, 1759–1770.
84. Bajard,L., Relaix,F., Lagha,M., Rocancourt,D., Daubas,P. and Buckingham,M.E. (2006) A novel genetic hierarchy functions during hypaxial myogenesis: Pax3 directly activates Myf5 in muscle progenitor cells in the limb. *Genes Dev.*, **20**, 2450–2464.
85. Ikram,M.S., Neill,G.W., Regl,G., Eichberger,T., Frischauf,A.M., Aberger,F., Quinn,A. and Philpott,M. (2004) GLI2 is expressed in normal human epidermis and BCC and induces GLI1 expression by binding to its promoter. *J. Invest. Dermatol.*, **122**, 1503–1509.
86. Agren,M., Kogerman,P., Kleman,M.I., Wessling,M. and Toftgard,R. (2004) Expression of the PTCH1 tumor suppressor gene is regulated by alternative promoters and a single functional Gli-binding site. *Gene*, **330**, 101–114.
87. Wu,S.M., Chien,K.R. and Mummery,C. (2008) Origins and fates of cardiovascular progenitor cells. *Cell*, **132**, 537–543.
88. Rho,J.Y., Yu,K., Han,J.S., Chae,J.I., Koo,D.B., Yoon,H.S., Moon,S.Y., Lee,K.K. and Han,Y.M. (2006) Transcriptional profiling of the developmentally important signalling pathways in human embryonic stem cells. *Hum. Reprod.*, **21**, 405–412.
89. Ingham,P.W. and McMahon,A.P. (2001) Hedgehog signaling in animal development: paradigms and principles. *Genes Dev.*, **15**, 3059–3087.
90. Takanaga,H., Tsuchida-Straeten,N., Nishide,K., Watanabe,A., Aburatani,H. and Kondo,T. (2009) Gli2 is a novel regulator of sox2 expression in telencephalic neuroepithelial cells. *Stem Cells*, **27**, 165–174.
91. Po,A., Ferretti,E., Miele,E., De Smaele,E., Paganelli,A., Canettieri,G., Coni,S., Di Marcotullio,L., Biffoni,M., Massimi,L. *et al.* (2010) Hedgehog controls neural stem cells through p53-independent regulation of Nanog. *EMBO J.*, **29**, 2646–2658.
92. Avilion,A.A., Nicolis,S.K., Pevny,L.H., Perez,L., Vivian,N. and Lovell-Badge,R. (2003) Multipotent cell lineages in early mouse development depend on SOX2 function. *Genes Dev.*, **17**, 126–140.
93. Graham,V., Khudyakov,J., Ellis,P. and Pevny,L. (2003) SOX2 functions to maintain neural progenitor identity. *Neuron*, **39**, 749–765.
94. Tukachinsky,H., Lopez,L.V. and Salic,A. (2010) A mechanism for vertebrate Hedgehog signaling: recruitment to cilia and dissociation of SuFu-Gli protein complexes. *J. Cell. Biol.*, **191**, 415–428.
95. Ohlmeyer,J.T. and Kalderon,D. (1998) Hedgehog stimulates maturation of Cubitus interruptus into a labile transcriptional activator. *Nature*, **396**, 749–753.
96. Goodrich,L.V., Johnson,R.L., Milenkovic,L., McMahon,J.A. and Scott,M.P. (1996) Conservation of the hedgehog/patched signaling pathway from flies to mice: induction of a mouse patched gene by Hedgehog. *Genes Dev.*, **10**, 301–312.
97. Doetschman,T.C., Eistetter,H., Katz,M., Schmidt,W. and Kemler,R. (1985) The in vitro development of blastocyst-derived embryonic stem cell lines: formation of visceral yolk sac, blood islands and myocardium. *J. Embryol. Exp. Morphol.*, **87**, 27–45.
98. Dyer,L.A., Makadia,F.A., Scott,A., Pegram,K., Hutson,M.R. and Kirby,M.L. (2010) BMP signaling modulates hedgehog-induced secondary heart field proliferation. *Dev. Biol.*, **348**, 167–176.
99. Sandmann,T., Jensen,L.J., Jakobsen,J.S., Karzynski,M.M., Eichenlaub,M.P., Bork,P. and Furlong,E.E. (2006) A temporal map of transcription factor activity: mef2 directly regulates target genes at all stages of muscle development. *Dev. Cell*, **10**, 797–807.
100. Tapscott,S.J., Davis,R.L., Thayer,M.J., Cheng,P.F., Weintraub,H. and Lassar,A.B. (1988) MyoD1: a nuclear phosphoprotein requiring a Myc homology region to convert fibroblasts to myoblasts. *Science*, **242**, 405–411.
101. Skerjanc,I.S., Slack,R.S. and McBurney,M.W. (1994) Cellular aggregation enhances MyoD-directed skeletal myogenesis in embryonal carcinoma cells. *Mol. Cell Biol.*, **1464**, 8451–8459.
102. Armour,C., Garson,K. and McBurney,M.W. (1999) Cell-cell interaction modulates myoD-induced skeletal myogenesis of pluripotent P19 cells in vitro. *Exp. Cell Res.*, **251**, 79–91.
103. Farah,M.H., Olson,J.M., Sucic,H.B., Hume,R.I., Tapscott,S.J. and Turner,D.L. (2000) Generation of neurons by transient expression of neural bHLH proteins in mammalian cells. *Development*, **127**, 693–702.
104. Dennler,S., Andre,J., Alexaki,I., Li,A., Magnaldo,T., ten Dijke,P., Wang,X.J., Verrecchia,F. and Mauviel,A. (2007) Induction of sonic hedgehog mediators by transforming growth factor-beta: Smad3-dependent activation of Gli2 and Gli1 expression in vitro and in vivo. *Cancer Res.*, **67**, 6981–6986.
105. Brewster,R., Mullor,J.L. and Ruiz i Altaba,A. (2000) Gli2 functions in FGF signaling during antero-posterior patterning. *Development*, **127**, 4395–4405.
106. Borycki,A., Brown,A.M. and Emerson,C.P. Jr (2000) Shh and Wnt signaling pathways converge to control Gli gene activation in avian somites. *Development*, **127**, 2075–2087.
107. Mizugishi,K., Aruga,J., Nakata,K. and Mikoshiba,K. (2001) Molecular properties of Zic proteins as transcriptional regulators and their relationship to GLI proteins. *J. Biol. Chem.*, **276**, 2180–2188.
108. McKinsey,T.A., Zhang,C.L. and Olson,E.N. (2001) Control of muscle development by dueling HATs and HDACs. *Curr. Opin. Genet. Dev.*, **11**, 497–504.
109. Ghosh,T.K., Song,F.F., Packham,E.A., Buxton,S., Robinson,T.E., Ronksley,J., Self,T., Bonser,A.J. and Brook,J.D. (2009) Physical interaction between TBX5 and MEF2C is required for early heart development. *Mol. Cell Biol.*, **29**, 2205–2218.
110. Vokes,S.A., Ji,H., Wong,W.H. and McMahon,A.P. (2008) A genome-scale analysis of the cis-regulatory circuitry underlying sonic hedgehog-mediated patterning of the mammalian limb. *Genes Dev.*, **22**, 2651–2663.
111. De Val,S., Anderson,J.P., Heidt,A.B., Khiem,D., Xu,S.M. and Black,B.L. (2004) Mef2c is activated directly by Ets transcription factors through an evolutionarily conserved endothelial cell-specific enhancer. *Dev. Biol.*, **275**, 424–434.
112. De Val,S., Chi,N.C., Meadows,S.M., Minovitsky,S., Anderson,J.P., Harris,I.S., Ehlers,M.L., Agarwal,P., Visel,A., Xu,S.M. *et al.* (2008) Combinatorial regulation of endothelial gene expression by ets and forkhead transcription factors. *Cell*, **135**, 1053–1064.
113. Visel,A., Minovitsky,S., Dubchak,I. and Pennacchio,L.A. (2007) VISTA Enhancer Browser–a database of tissue-specific human enhancers. *Nucleic Acids Res.*, **35**, D88–D92.
114. Skerjanc,I.S. and Wilton,S. (2000) Myocyte enhancer factor 2C upregulates MASH-1 expression and induces neurogenesis in P19 cells. *FEBS Lett.*, **472**, 53–56.
115. Morin,S., Pozzulo,G., Robitaille,L., Cross,J. and Nemer,M. (2005) MEF2-dependent recruitment of the HAND1 transcription factor results in synergistic activation of target promoters. *J. Biol. Chem.*, **280**, 32272–32278.
116. Morin,S., Charron,F., Robitaille,L. and Nemer,M. (2000) GATA-dependent recruitment of MEF2 proteins to target promoters. *EMBO J.*, **19**, 2046–2055.
117. Ieda,M., Fu,J., Delgado-Olguin,P., Vedantham,V., Hayashi,Y., Bruneau,B. and Srivastava,D. (2010) Direct reprogramming of fibroblasts into functional cardiomyocytes by defined factors. *Cell*, **142**, 375–386.
118. Toro,R., Saadi,I., Kuburas,A., Nemer,M. and Russo,A.F. (2004) Cell-specific activation of the atrial natriuretic factor promoter by PITX2 and MEF2A. *J. Biol. Chem.*, **279**, 52087–52094.